CHALMERS
UNIVERSITY OF TECHNOLOGY

Stone Columns in Extremely Soft Soils in Scandinavia

Master's thesis in the Master´s Program Infrastructure and Environmental Engineering

KHADEEN SALEH

DEPARTMENT OF Architecture and Civil Engineering
Division of Geology and Geotechnical Engineering

CHALMERS UNIVERSITY OF TECHNOLOGY
Gothenburg, Sweden 2024
www.chalmers.se
Master's Thesis

DEPARTMENT OF Architecture and Civil Engineering
CHALMERS UNIVERSITY OF TECHNOLOGY
Gothenburg, Sweden 2024
www.chalmers.se

CHALMERS
UNIVERSITY OF TECHNOLOGY

MASTER'S THESIS ACEX99

Stone Columns in Extremely Soft Soils in Scandinavia

Master's Thesis in the Master's Programme Infrastructure and Environmental Engineering

KHADEEN SALEH

Department of Architecture and Civil Engineering
Division of Geology and Geotechnical Engineering
Research Group of Geotechnical Engineering
CHALMERS UNIVERSITY OF TECHNOLOGY
Gothenburg, Sweden 2024

Stone Columns in Extremely Soft Soils in Scandinavia

Master's Thesis in the Master's Programme Infrastructure and Environmental Engineering

KHADEEN SALEH

© KHADEEN SALEH, 2024

Examensarbete ACEX99
Institutionen för arkitektur och samhällsbyggnadsteknik
Chalmers tekniska högskola, 2024

Department of Architecture and Civil Engineering
Division of Geology and Geotechnical Engineering
Research Group of Geotechnical Engineering
Chalmers University of Technology

SE-412 96 Göteborg
Sweden
Telephone: + 46 (0)31-772 1000

Stone Columns in Extremely Soft Soils in Scandinavia

Master's thesis in the Master's Programme Infrastructure and Environmental Engineering

KHADEEN SALEH

Department of Architecture and Civil Engineering
Division of Geology and Geotechnical Engineering
Research Group of Geotechnical Engineering
Chalmers University of Technology

ABSTRACT

Stone columns are a well-established technique for improving the properties of soil under the foundation of embankments and heavy structures. Stone columns are inclusions of granular material typically installed using vibratory-displacement or vibro-replacement methods. A notable advantage of stone columns is that they tend to have a minimal impact on the properties of the surrounding soil, unlike other ground improvement methods. The primary outcomes of stone columns in untreated soil conditions include improved bearing capacity, reduced total and differential settlements, accelerated consolidation, enhanced stability of embankments and natural slopes, and decreased liquefaction susceptibility. Stone columns function as inclusions that provide higher stiffness, shear strength, and permeability than the natural soil. This enables them to effectively support the structure or embankment without significantly altering the physical state of the surrounding soil, as well as improve the drainage.

The research aims to examine whether stone columns can be used in the soft clays typical to Scandinavia, resulting in preliminary design graphs. The numerical simulations will be carried out using constitutive models such as Creep-SCLAY1S and Soft Soil under 2D axisymmetric conditions in Plaxis. The simulations will be done as fully coupled consolidation concerning typical soil characteristics in Scandinavia. Ultimately, the outcome of this study would include Priebe-type charts suitable for Scandinavian clay, which can assist designers in constructing stone columns in each area.

The findings reveal a substantial effect of the chosen constitutive model, the influence of replacement ratio A/A_c (the ratio of the area of the stone column to the area of the soil it replaces)**,** and the effective friction angle of the stone column material on the settlement improvement factor. Furthermore, the results confirm and build upon previous findings, indicating that creep and increasing lateral earth pressure K increase the settlement improvement factor. Consequently, the results can be applied in stone column design for highly soft clay conditions (such as Swedish soil), where using Priebe's charts might not be applicable.

Key words: creep, extremely soft soil, friction angle, replacement ratio, Creep-SCLAY1S, settlement improvement factor, Soft Soil, Soft Soil-creep, and stone columns.

Table of Content

Preface

This master thesis was carried out between January and June 2024 at the Department of Civil and Environmental Engineering, Geology and Geotechnical Division, at Chalmers University of Technology, Sweden.

I would like to thank my examiner Prof. Minna Karstunen and Keller Grundläggning AB for their support and guidance during this project.

Göteborg June 2024

Khadeen Saleh

Notations

List of Letters

a_d	Deviatoric fabric tensor
a_s	Area replacement ratio
$c´$	Effective cohesion
k	Constant depends on the column arrangement
n	Settlement improvement factor
n_s	Stress concentration factor
$p´$	Mean effective stress
p	Mean stress
$p´_0$	Isotropic pre-consolidation stress
p^{eq}	Actual stress state
$p_p{}^{eq}$	Equivalent pre-consolidation stress
$p´_m$	Effective stress of actual yield surface
q_c	Tip resistance
r_c	Radius of stone column
s_t	Settlement in reinforced ground (at a given time)
s_0	Settlement in untreated ground
A	Effective area (Unit cell area)
A_c	Area of stone column
C_u	Undrained shearing resistance
C_α	Creep index
D_c	Stone column diameter
D_e	Effective diameter
E_{oed}	Oedometric soil modulus
E_{ur}	Loading, reloading soil modulus
E_s	Young's modulus of soil
E_c	Young's modulus of column
K	Lateral earth pressure
K_0	Lateral earth pressure at rest
K^*	Lateral earth pressure coefficient
L_c	Length of stone column
M	Slope of Critical state line (CSL)
N_{SPT}	Standard penetration test
S	Stone column spacing

List of Symbols

$\sigma'_v = \sigma'_1$	Vertical effective stress
σ'_h=σ'_3	Horizontal effective stress
τ_f	Effective shear stress in failure plane
σ'_{nf}	Effective normal stress in failure plane
ε_p^c	Plastic strain
$\sigma´_r$	Effective radial stress
$\sigma´_a$	Effective axial stress
σ_s	Stress in soil of unit cell
σ_c	Stress in column
σ_d	Deviatoric stress

φ'	Effective friction angle
ϑ_1	Virgin consolidation
ϑ_s	Swelling line
$d\varepsilon_v^P$	Increment of plastic volumetric strain
ν	Poisson ratio
k	Hydraulic conductivity
λ	Compression index
λ^*	Modified compression index
λ_i	Inclination of the normal compression plane
λ_i^*	Modified intrinsic compression index
κ	Swelling index
κ^*	Modified swelling index
ε_v	Volumetric strain
ε_v^e	Elastic volumetric strain
ε_v^P	Plastic volumetric strain
ε_c^H	Deformation during consolidation
μ^*	Modified creep index
τ_c	Parameter related to geometry and consolidation
η	Tensional equivalent for stress ratio =q/p´
χ	Amount of bonding
ω	Rate of rotation
ω_d	Rate of rotation due to deviator strain
ξ	Absolute rate of destructuration
ξ_d	Relative rate of destructuration
α_0	Initial value of anisotropy
α	Scalar value of anisotropy
α_d	Deviatoric fabric tensor
β	Creep exponent
ε_a	Axial strain
ε_r	Radial strain
ε_v	Volumetric strain
ε_q	Deviatoric strain
$\dot{\varepsilon}$	Strain rate
$\dot{\varepsilon}^{\,e}$	Elastic strain rate
$\dot{\varepsilon}^{\,c}$	Creep strain rate
ε_ϑ^e	Volumetric elastic strain rate
ε_q^e	Deviatoric elastic strain rate
$d\varepsilon_d$	Incremental deviatoric strain tensor
θ_α	Loade angle
η_0	Stress ratio corresponding K_0 state
Δt	Time increment
τ	Reference time
$M(\theta)$	Stress ratio at critical state
M_e	Stress ratio at critical state in triaxial extension
M_c	Stress ratio at critical state in triaxial compression
$(J_2)_\alpha$	Modified second invariant to a-line
$(J_3)_\alpha$	Modified third invariant to a-line

1. Introduction

Ground improvement involves techniques to modify the soil used in earthworks or the foundation soils, enhancing their performance under design and operational loading conditions (Schaefer et al., 2012). With the increased construction of embankments and heavy structures on weak soils, there is a growing demand for ground improvement techniques (Castro et al., 2013). Consequently, ground improvement methods have significantly evolved over the past fifty years and are now integral to various geotechnical and construction designs (Schaefer et al., 2012).

Numerous methods and technologies are employed in ground improvement to alter the soil properties, when removing existing soil is not feasible due to cost, environmental, and technical constraints (Schaefer et al., 2016). Mitchell (1981) classified ground improvement applications into categories such as compaction for densification of in-situ cohesionless soil, consolidation via preloading and/or vertical drains, grouting, soil stabilisation using admixtures, thermal stabilisation, and soil reinforcement. Chu et al. (2009) proposed five methods for ground improvement: non-cohesive soil non-admixtures inclusion, fine-grained soil improvement without admixtures, inclusions, grouting admixtures, and earth reinforcement.

The selection of an improvement method for a specific project is a complex process that involves meeting the requirements of ground improvement for a given project. Factors such as geometry, density, settlement, stability, and others are considered crucial in the design process. Additionally, surface conditions, loading conditions, materials, and construction techniques can influence the choice of method (Schaefer et al., 2012). Figure 1 provides a visual representation of the appropriate technique for various soil types. While some techniques have well-established design procedures, others are currently under development or have proprietary design processes (Schaefer et al., 2012).

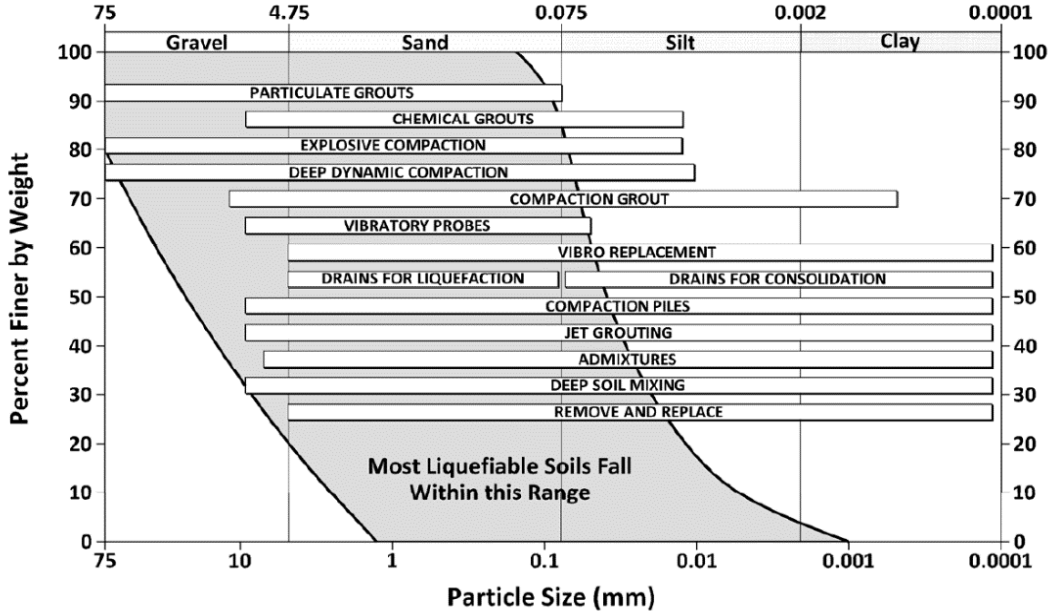

Figure 1: The suitable ground improvement techniques for various types of soil (Schaefer et al.,2012)

It has been demonstrated through decades of experience that the required performance of these applications, such as the improvement in bearing capacity, slope stabilisation, precompression and acceleration of consolidation, and the construction of seepage barriers, can be obtained if the appropriate ground improvement method is chosen for the problem, and if both design and construction are done well. One frequent critical aspect of most approaches is the challenge of confirming that the intended degree of improvement has been achieved (Schaefer et al., 2012).

Stone columns are an innovative and widely utilised technique, which offers a promising solution for improving soil properties. This method, often employed on soil that is unsuitable for construction purposes (Castro, 2017), involves creating vertical columns of compacted aggregate using a vibrator, known as the vibro-replacement or vibro-displacement method, to enhance the characteristics of the soil.

Typically, a significant number of columns, or groups of columns, are installed when employing stone columns. However, it is essential to note that stone columns may not be suitable for highly sensitive soils, as found in Scandinavia, as maintaining the continuous stability of the columns and their geometric shape could be problematic.

Finally, selecting the appropriate ground improvement technique for a specific problem is a sophisticated procedure influenced by multiple factors. This complexity can make obtaining the desired outcomes from the employed techniques challenging.

1.1. Case study

Constructing stone columns in extremely soft soil poses significant challenges. Inadequate lateral support of the surrounding soil, among other factors related to soil properties, can compromise the intended load-bearing capacity of the stone columns. This scenario necessitates further exploration into the behaviour of stone columns in very soft soil conditions.

Considering the Ønsoy clay in Norway as a representative of medium sensitive clay in Scandinavia (Berre, 2014; Berre, 2018), this study investigates the possible settlement improvement by stone columns in Ønsoy clay using Plaxis 2D software for numerical model simulation.

1.2. Aim

Examine whether stone columns can be used in typical Scandinavian medium sensitive clays and present preliminary design recommendations.

1.3. Objectives

The objectives of this thesis will be as follows:

1. A literature review on the application of stone columns in extremely soft supported by previous case studies by Keller, a specialist ground engineering company with wide experience in ground improvement applications both internationally and in Scandinavia.
2. Understanding the installation procedure and how it may affect the performance.
3. Investigating the impact of K_0 (the earth pressure coefficient at rest), as that will change due to installation.

4. Critical evaluation of constitutive models for the design of stone columns, and their ability to be applied in Scandinavian soil conditions.
5. Using constitutive models such as the Creep-SCLAY1S and Soft Soil model in systematic numerical simulations, employing 2D axisymmetric conditions in Plaxis. The modelling will be performed as a fully coupled consolidation
6. The result: Priebe type diagram for Scandinavian ground conditions and design guidance.

1.4. Limitations

- This study will not simulate the installation effects of stone columns in sensitive clay. Instead, the installation effects will be considered via a comprehensive literature review, as well as considering the increase in the earth pressure at rest K_0 due to installation to be equal to one.

- The study will not examine the influence of creep on the response of the stone column material, only creep in the soft clay will be considered.

2. Background

Stone columns, also called granular columns or aggregate piers, stand out as one of the most extensively utilised ground improvement techniques. They are made of gravel-filled vertical holes in the soil that have been vibrated into a compacted form (Castro, 2014). The popularity of stone columns stems from their simplicity, ease of implementation, and relatively low cost, factors highly favoured by professional engineers (Dash & Bora, 2013). In challenging foundation sites, stone columns play a crucial role in enhancing various aspects such as boosting bearing capacity, reducing overall and differential settlements, accelerating consolidation, improving the slope stability of embankments, and fortifying the resistance to liquefaction (Barksdale & Bachus, 1983; Castro, 2014).

The effectiveness of stone columns in enhancing weak soil is due to two main factors. First, the stiff column material, such as gravel and crushed stones, is added to the soft soil. Second, the surrounding soil is densified during the installation of the Vibro-compacted stone column itself, followed by subsequent consolidation in the weak soil before the final loading of the improved ground (Guetif et al., 2007).

According to Mitchell (1981), the construction of stone columns involves replacing a segment of unsuitable soil with vertical columns of compacted stone, typically extending through the entire thickness of weak strata. This process usually results in a stiffer composite material with lower compressibility and higher shear strength than the original soil.

Generally, stone columns replace 15 to 35% of the volume of the soft soil during construction. When vertical loads are applied at the ground surface, the weak soil and the stone columns settle, leading to a significant stress concentration within the stone column (Golakiya & Lad, 2015).

Stone columns are commonly used to support low-rise constructions such as raft foundations, liquid storage tanks, and embankments, mainly when situated a top of loose silty sands containing over 15% fine particles, or in other very soft to hard fine-grained soils. The ideal soil conditions for applying stone columns are clayey soils with an undrained shear strength ranging between 15 and 50 kPa (Barksdale & Bachus, 1983).

2.1 Stone column construction method

To construct stone columns, a hole is created in the ground and filled with granular material. Achieving the desired strength of the stone column involves compacting the granular fill, typically comprised of stone or a blend of stone and sand in the appropriate proportions, utilising suitable compaction techniques. Various methods have been employed to install stone columns, considering their effectiveness and the availability of required equipment in the vicinity (Mitchell, 1981).

However, the successful improvement of soft and very soft soil depends upon the careful selection of stone column construction methods and their meticulous on-site

execution (McCabe et al., 2009). The most commonly applied methods for stone column construction include:

2.1.1. Vibro-replacement method

This method is typically employed when dealing with fine-grained soils. A vibrator is used to create a hole that is filled with granular material and compacted with the vibrator. The primary advantages of this method include its depth and speed of execution (Piccinini, 2015). In the application of this method for constructing stone columns, both wet and dry methods can be applied:

- Wet-top feed method: This involves lowering a probe with the help of water to the desired depth, creating a hole in the ground. Once the uncased hole reaches the appropriate depth, it is flushed out, and then stone backfill, ranging in size from 12 to 75 mm, is added incrementally at intervals of 0.3 to 1.2 m. Refer to Figure 2. Subsequently, an electrical or hydraulic vibrator compacts the backfill at the probe's bottom (Piccinini, 2015). This technique suits soft, fine-grained, and moderately impervious soil (Dheerendra Babu et al., 2013). Additionally, it is applicable for medium and deep treatment, having been successfully employed in soft clay soil (McCabe et al., 2009).

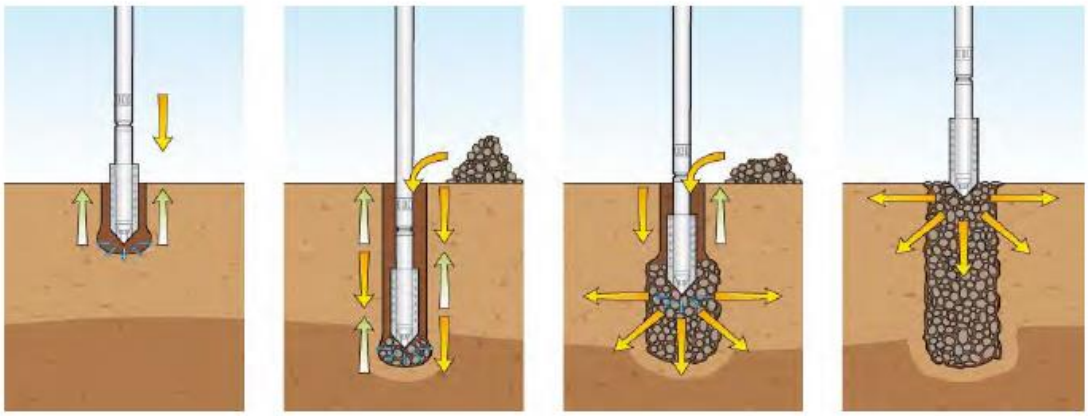

Figure 2: Stone columns construction, Wet-top feed technique. (Taube,2001).

- Dry-top feed method: The critical distinction between the dry and wet processes lies in the absence of water jetting during hole creation. See Figure 3. Unlike the wet process, the dry method maintains the vibrated hole open after the probe is withdrawn. Therefore, it is only suitable for application in stable, insensitive fine-grained soils with an undrained shear strength ranging between 30 and 60 kPa, excluding very soft clay (Babu et al., 2012). As per McCabe et al. (2009), this approach can be used for shallow to medium-depth granular columns typically designed to support light to heavy loads.

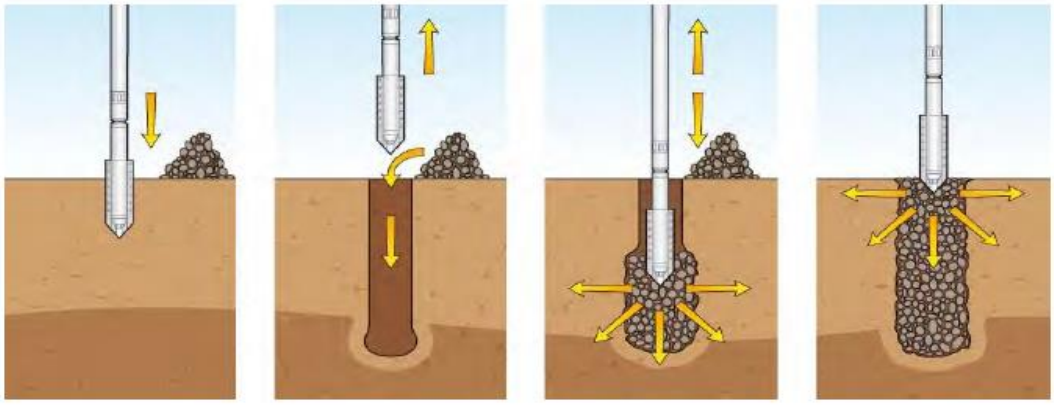

Figure 3: Stone columns construction. Dry-top feed technique. (Taube,2001).

- Dry-bottom feed method: Since its development in the 1970s, this technique has seen widespread adoption (McCabe et al., 2009). Its creativity lies in the vibrator's ability to facilitate stone column installation in areas characteried by high groundwater levels and soft soils. Through eccentric tubes positioned beside the probe, delivery of stone, sand, or concrete to the bottom of the excavated hole can be achieved without necessitating vibrator removal. Refer to Figure 4. In this method, the vibrator serves as a shield, preventing hole collapse (Piccinini, 2015). Wehr (2013) has documented numerous instances of successful stone column implementation in very soft soil conditions, mainly when the undrained shear strength (C_u) falls within the range of 4 to 5 kPa.

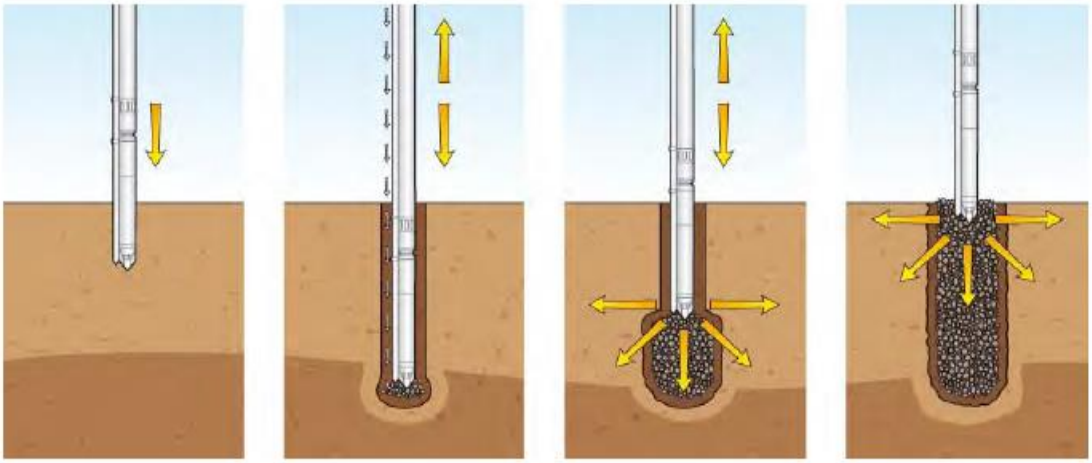

Figure 4: Stone column construction. Dry-bottom feed technique. (Taube,2001)

2.1.2. Vibro-composer method

Originating from Japan, the Vibro-composer method applies to stabilizing soft clays, particularly in abundant groundwater. Compacted columns are constructed to reach the desired depth by utilising a large vertical vibratory hammer atop a casing pipe. Subsequently, after adding a predetermined quantity of sand, the vibratory hammer is employed to extract and partially drive the casing from the bottom alternately. This process repeats until a fully compacted granular column is formed. This method is suitable for constructing columns with diameters ranging from 0.6 to 0.8 metres (Babu et al., 2012).

2.1.3. Rammed Columns

This method entails gradually compacting granular materials into pre-bored holes using a heavy falling weight, typically ranging from 15 to 20 kN, with a drop height of 1.0 to 1.5 metres. While considered a viable alternative to vibrator compaction, this method yields stone columns with greater capacity compared to those produced by vibro-float. However, its application is limited in soft soil due to disturbance and subsequent remoulding caused by the ramming operation. It becomes impractical when the depth of stone columns exceeds 12 metres (Babu et al., 2012).

2.2. Basic design factors

Various design factors affect the capacity of stone columns to hold loads. The following are the main factors that define the capability of stone columns:

1. Column diameter

The diameter of stone columns (D_c) typically ranges from 0.4 to 1.2 metres. However, factors such as the desired level of improvement, installation technique, stone size, and the strength of the in-situ soil all play a role in determining the specific diameter of the column (Golakiya & Lad, 2015). In soft, fine-grained soils where stone columns are installed, the process tends to self-adjust; the softer the soil, the larger the diameter of the resulting stone column (Ranjan, 2016).

The final diameter of the hole is invariably larger than the initial diameter of the probe or casing. This is due to the lateral displacement of stones during vibration or ramming (Ranjan, 2016). That is influenced by factors such as soil type, undrained shear strength, stone size, vibrating probe or rammer characteristics, and the construction methodology employed. Understanding the role of soil type and stone size in this process is key to comprehending the construction methodology.

2. Distribution pattern of columns

Stone columns can be arranged either in a square formation or in a triangular configuration, as shown in Figure 5. While a square pattern is sometimes used, equilateral triangles are more frequently employed for constructing stone columns. Within a given area, the highest concentration of stone columns is typically observed within the equilateral triangle arrangement rather than the square arrangement (Golakiya & Lad, 2015).

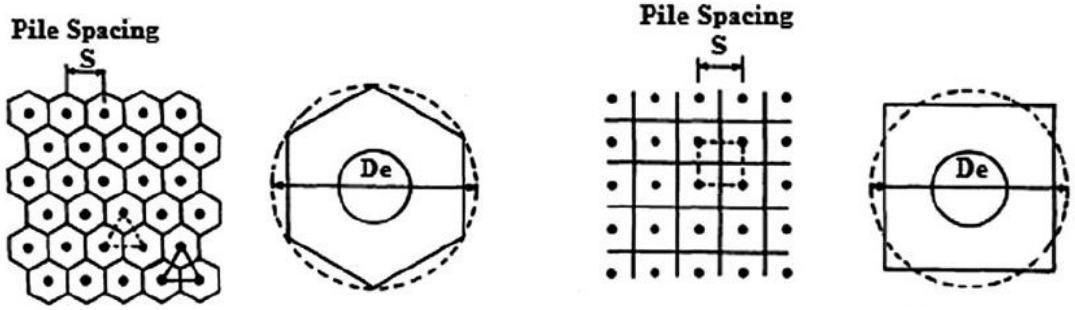

Figure 5: Stone column installation patterns, the triangular one to the left and the square one to the right.

3. Column spacing

The spacing between stone columns at maximum and minimum distances is determined based on the site-specific conditions. However, column spacing, denoted by S, can be defined considering site characteristics, loading patterns, column material properties, installation methods, and settlement tolerances. According to Sondermann et al. (2016), the spacings range between 1.5 and 2.5m, while Babu et al. (2012) referred to the spacing as 2 to 3 times the diameter of the column. In the meantime, field tests are recommended for large-scale projects to determine the optimal stone column spacing, considering the allowable settlement of the foundation and the required bearing capacity of the soil (Golakiya & Lad, 2015).

For settlement and stability calculations, it is advisable to treat the surrounding soil area of each stone column as an equivalent circle with the same total area. This equivalent circle has an effective diameter (D_e) of 1.05S for an equilateral triangular arrangement of columns and 1.13S for a square grid (Babu et al., 2012). This unit cell represents an equivalent cylindrical volume of material with a diameter of D_e, encompassing one stone column and the adjacent soil (Babu et al., 2012).

4. Area replacing ratio (ARR)

The extent to which stone columns replace soil directly influences the performance of the improved ground. The Area Replacement Ratio (ARR) quantifies this effect by comparing the area of the compacted stone column (A_c) to the total area within the unit cell (A) (Sexton et al., 2013). As shown in Figure 6.

Research by Shahu et al. (2011) indicates that increasing the replacement area ratio enhances the overall response of ground reinforced with granular columns. A minimum area replacement ratio of 0.25 is deemed necessary for observing a noticeable increase in bearing capacity in the enhanced ground by stone columns (Wood et al., 2000).

$$a_s = A_c/A = (D_c/D_e)^2 = \frac{1}{k}\left(\frac{D_c}{S}\right)^2 \qquad \textit{Eq. (1)}$$

where a_s is the area replacement ratio, A_c is the area of stone column, A is the area within the unit cell, D_c is the diameter of stone column, D_e is the effective diameter,S is the spacing between columns, and k is a constant depends on the column arrangement (see Fig. 6).

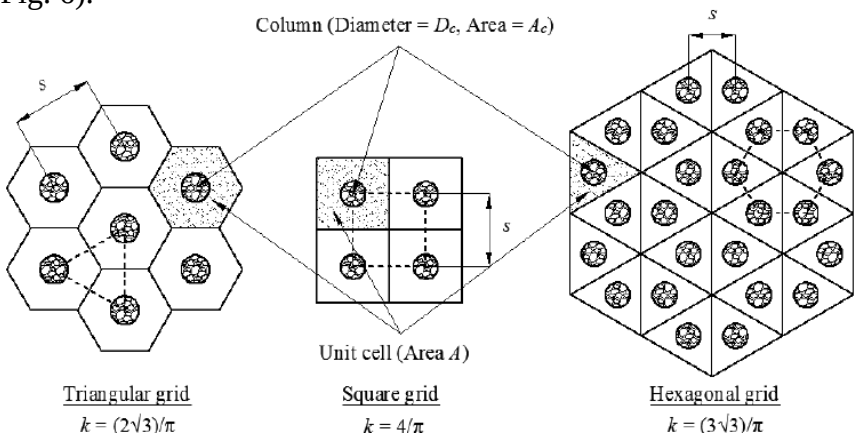

Figure 6: The Area replacement ratio for stone columns (adapted from Sexton et al., 2015)

5. Stress concentration ratio (SCR)

The stone column material exhibits significantly greater stiffness compared to the surrounding soil. According to principles of equilibrium, the stress within the surrounding soil should ideally be lower than that within the strongest stone columns, resulting in stress concentration within the granular column. The stress concentration ratio (n_s) resulting from an externally applied load (σ_p) is defined as the ratio of the average stress in the stone column (σ_c) to the stress in the soil (σ_s) within the unit cell (Golakiya & Lad, 2015). As represented by Equation (2).

$$n_s = \sigma_c / \sigma_s \qquad \textit{Eq. (2)}$$

According to Goughnour and Bayuk (1979), typical values of n_s range between 3 and 6 for stone column friction angles of 30° and 45°, respectively, at the ground level and falling between 3 and 4.5 at a depth of the column. Similarly, Juran and Guermazi (1988) observed that the stress concentration factor increases at the surface and decreases along the length of the stone column; simultaneously, it increases with consolidation time.

2.3. Stone columns in extremely soft clay

Very soft clay can be characterised by several specifications, such as a standard penetration test (N_{SPT}) value of less than 2, an undrained shear strength C_u of less than 20 kPa, and a tip resistance (q_c) of less than 1 MPa (Almeida et al., 2022).

Consequently, due to their unique structural characteristics—high water content, low shear strength, and low permeability—geotechnical structures constructed on soft soil require careful consideration (Wassie & Demir, 2023).

Generally, soils with undrained shear strengths of less than 15 kN/m² exhibit an excessive tendency for compressibility and creep. So, applying excessive structural load to such weak soils may result in excessive pore pressures, thus causing problems with stability and leading to significant deformations. Consequently, structures built on soft soils are particularly vulnerable to severe deformations and slope failures, especially deep-seated failures (Deshpande et al., 2021).

Utilising the stone column method to improve very soft clay soil enhances its load-bearing capacity. Extending the penetration length of the columns also increases the bearing capacity of the soil (Malarvizhi & Ilamparuthi, 2007). Wassie and Demir (2023) noted that extending the length of the granular columns from half the embankment height to the full height reduces excess pore water pressure by half. However, extending the columns beyond the necessary length improves settlement performance but does not necessarily enhance bearing capacity performance (Grizi et al., 2022). However, Castro (2017) indicates that the stone columns, with a length beyond the critical one, do not make a remarkable improvement in both settlement and soil-bearing capacity.

The value of the critical length of the columns can be discrepant, as it is sometimes provided as a function of the load. This illustrates that the footing dimensions

significantly influence the critical length of the columns. A few more column modelling-related elements, such as the impact of column installation, are also discussed (Castro, 2017).

Nevertheless, McCabe et al. (2009) and Basack et al. (2016) highlighted that undrained shear strength C_u increases permanently during granular column construction. At the same time, the lateral stresses increase due to the process of column installation. However, applying granular columns to improve the soil may not be effective if the shear strength of the embankment soil is less than that of the foundation soil (Prakash & Krishnamoorthy, 2022).

Nonetheless, settlements decrease as the ratio of stone column length to its diameter (L_c/D_c) increases until it reaches a value of 10 (Malarvizhi & Ilamparuthi, 2007). Castro (2017) mentioned that the efficient column length is twice the foundation width (B) in homogenous soft soil. Moreover, Wassie and Demir (2023) noted that doubling the length of the stone columns reduces settlement by two-thirds. Sarvaiya and Solanki (2015) found the most effective L_c/D_c ratio is between 4 and 5, and thus increasing the ratio does not yield further improvement beyond this point.

On the other hand, as the internal effective friction angle φ' of the stone columns increases, the settlements decrease. However, when the applied load is relatively small, and the effective friction angle is approximately $\varphi' \approx 32°$, the settlement reduction ratio is almost equal to one. This indicates that using loose gravel or crushed stone is inadequate to increase the load-bearing capacity (Malarvizhi & Ilamparuthi, 2007).

According to McCabe et al. (2009), the Priebe design model, which utilizes commonly used effective friction angle of $\varphi' \approx 40°$, offers a reliable lower-bound approximation of bottom-feed performance. Although it does not fully consider the fundamental changes in the soil and the stress changes occurring during granular column construction and load application, leading stone column designers still rely on this method due to its reliability.

Bulging is the most common failure mechanism for stone columns, mainly when the confining stress is lower than the applied load. It typically occurs at the top of granular columns as the confining stress increases with depth (Idrus et al., 2023). Barksdale and Bachus (1983) suggested that bulging of the stone column may occur at a depth of two to three times D_c, while Malarvizhi and Ilamparuthi (2007) mentioned that it occurs at a depth of four times D_c from the ground surface.

Prakash and Krishnamoorthy (2022) noted that column clogging significantly delays the consolidation and settlement of soft clay. Furthermore, the drainage capacity of columns is influenced by factors such as the capture coefficient (it is a function of flow velocity and increases with flow velocity increasing, where it can be defined according to Gruesbeck and Collin (1982) equation), area ratio, critical hydraulic gradient (which can be determined by calculating the discharged water and the eroded mass of the soil, where the thickness of the clay layer, spacing between columns, and effective friction

angle influence its value), compressibility ratio, and permeability ratio (Pal & Deb, 2019).

Stone column blockage is more common at lower ratios of volume compressibility than at higher ratios. Additionally, the probability of stone column blockage increases with decreasing critical hydraulic gradient, area ratio, and permeability ratio of the clay fine particles. Generally, a blocked stone column may result in greater final settlement but a slower consolidation rate (Tai & Zhou, 2019).

2.4. Stone columns application in extremely soft clay

The potential applications of stone columns include mitigating soil liquefaction, supporting retaining structures (such as reinforced earth), enhancing the stability of embankments, reinforcing foundation soils beneath embankments and fills, and providing support for bent (pier) and abutment structures for bridges on loose silty sands and moderately soft to stiff clays (Prasad & PVV, 2016). In instances where a relatively significant settlement is tolerable, such as for the foundations of large structures like liquid storage tanks, earthen embankments, and raft foundations, stone columns can effectively increase bearing capacity and reduce settlement. Additionally, stone columns can expedite primary consolidation (Prasad & PVV, 2016).

The most effective application of stone columns is to densify clean, non-cohesive soils. However, according to Mitchell (1981), granular columns may not perform well when the percentage of fines—particles smaller than 200 mesh sieve or 0.074mm—exceeds 20 to 25 percent by weight. This is explained by particles contribution to cohesion, making column construction challenging. Additionally, materials with more significant fine percentages may have limited permeability that impedes quick pore water drainage, which is required to densify liquified soil following stone column installation (Mitchell, 1981).

Prasad and PVV (2016) noted that stone columns may not receive sufficient lateral confinement from the surrounding soil in very soft soils, leading to inadequate load-bearing capacity. Nonetheless, stone columns can influence loose, sandy soils below the water table to mitigate liquefaction during earthquakes.

However, limitations exist when using stone columns in sensitive clays due to the absence of lateral constraints. This results in faster settlement of the bed layer and reduced radial drainage caused by clay particles trapping around the stone columns (Malarvizhi & Ilamparuthi, 2004).

According to Emam et al. (2022), the application of stone columns is prohibited if the soil has an undrained shear strength of C_u < 15 kN/m². However, adding confinement and encasing individual granular columns with geosynthetics is beneficial for enhancing stone column performance in highly soft soils.

Wehr et al. (2008) discussed three projects in Sweden that were built on highly soft soil. For instance, in Frövifros, grouted stone columns with a diameter of 75cm were utilised when the undrained shear strength ranged from 8 to 14 kPa. Vibro-gravel drains

with short lifts of 1m were deemed essential to prevent liquefaction during the construction of grouted stone columns.

Furthermore, Wehr (2013) discovered, through four conducted lab tests, that there was no failure during column installation when the undrained shear strength of the soil was C_u=4 kN/m^2 and the water content was at 30.5%, even when the static weight doubled from 40 to 80 N. However, the failure of stone columns occurred when C_u decreased to 3.5 kN/m^2, and the water content increased to 32%. This failure coincided with the doubling of the diameter of the granular columns, causing the soil stresses at the surface to become insufficient to support the column. Adherence to the European standard EN 14731 for monitoring and testing, along with utilising a bottom feed system with an adjustable vibrator frequency, was deemed crucial in such scenarios (Wehr et al., 2008).

3. Lateral earth pressure (*K*)

A primary factor contributing to stone column construction in the soil is the positive impact of vibro-installation process on the stress state of the soil. Therefore, utilising vibro-installation technique to insert stone columns into weak soil transcends a mere soil replacement procedure, as this installation method induces horizontal shifting and vibration in the soil (Elshazly et al., 2005).

Since lateral earth pressure influences column yielding and provides a degree of lateral support, it plays a significant role in the improvement factor achieved with a stone column treatment. Thus, the *K* value, representing lateral earth pressures, becomes a critical parameter in stone column design (Camelo, 2016).

Installing stone columns disturbs the surrounding soil, particularly when the displacement method is employed, altering the characteristics of soft soil. The introduction of columns elevates the horizontal stresses of the soil concerning, leading to an increase in the lateral earth pressure coefficient (*K**). This augmentation in effective horizontal stresses, observed after the consolidation phase and cavity expansion, contributes to the beneficial effects of column installation in soft soils (Castro & Karstunen, 2010). However, disregarding radial stress variations may result in overestimating settlements associated with stone columns and underestimating the effectiveness of their ultimate capacity (Elshazly et al., 2005).

Castro and Karstunen (2010) highlighted that plotting the lateral earth coefficient reveals a plateau at 4-8 times the column radius (r_c) from the column's centreline. As depicted in Figure 7, this value should be regarded as the lateral earth stress value once the pore pressures generated during construction have dissipated.

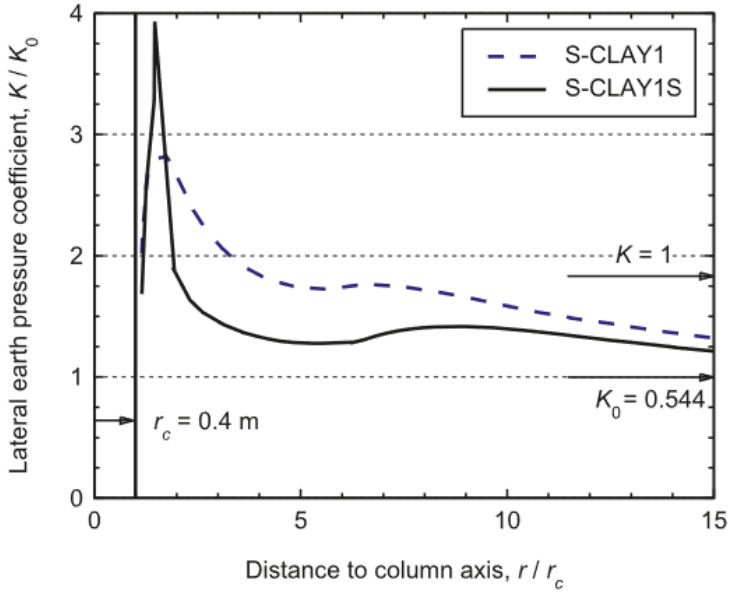

Figure 7: Change in lateral earth coefficient versus distance from the column centre (adapted from Castro & Karstunen, 2010).

Moreover, the numerical results that have been obtained from Castro and Karstunen (2010) FEM model and Kirsch (2004,2006) field study have a similar trend. The

differences may also be due to remoulding and dynamic impacts that were not considered in the model by Castro & Karstunen (2010). See Figure 8.

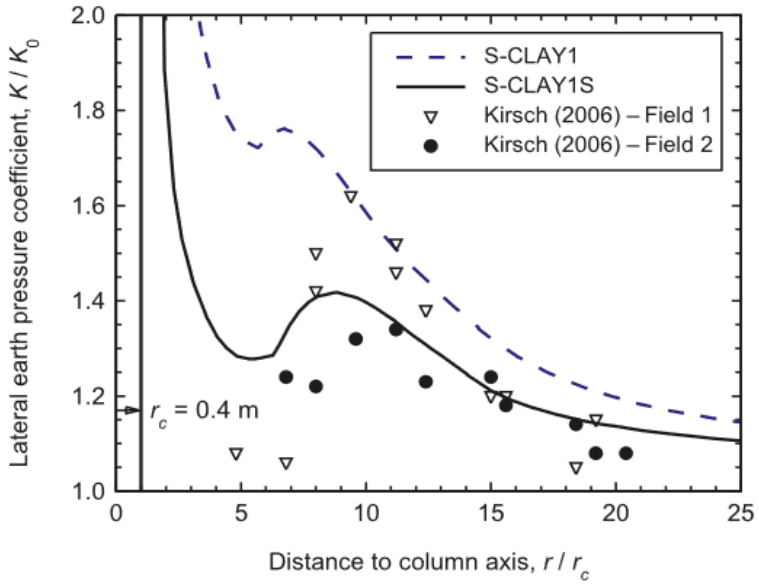

Figure 8: K value of FEM modelling versus Kirsch 2006 field results (adapted from Castro & Karstunen, 2010).

Shehata et al. (2018) observed that the most significant impact of lateral earth pressure occurs within 1 to 3 times the column radius (r_c) from the column centre. Subsequently, horizontal movement decreases in a zone spanning 4-8 times the column radius, resulting in reduced densification. However, beyond eight times the radii, the influence of stone column installation diminishes entirely.

Guetif et al. (2007) noted that the anticipated increase in effective radial stress in soft clay leads to a significant decrease in lateral strains. Consequently, the coefficient of lateral earth pressure at rest (K_0) rises progressively from the outset and approaches a value of one near the column. In calculating settlement in the original soil, Priebe assumed a hydrostatic state (K_0=1) following stone column installation. According to Camelo (2016), the lateral stress coefficient increases from K_0 to nearly 2.3 K_0 beside the column. However, the overall impact of granular column installation on K_0 disappears within 11 times r_c.

Shien (2013) highlighted that the effect of column installation is more pronounced at the column boundary, approximately 3.2 times K_0, within the installation zone, extending to 12 times r_c (see Figure 9). This observation aligns closely with the field measurements by Kirsh (2006), indicating the reliability and consistency of the findings. Furthermore, Carvajal et al. (2013) emphasised that the lateral earth pressure value is the most reliable indicator for assessing soil improvement post-stone column installation. Assessing K can be achieved by comparing the cone penetration resistance after stone column installation to the tip resistance before the column construction at the field. Additionally, the value of K/K_0 ranges between 1.5 and 2, with the influence diameter measuring 4 to 6 times r_c at a depth of 16 metres and between 10 and 14 radii at a depth of 6 metres. However, as the column spacing of 1.5 to 2.5 metres that means the impact of the stone column installation will primarily affect the unit cell itself, rather

than extending beyond its boundaries. Additionally, the overlap of the influence zones of adjacent stone columns may lead to increased stress concentrations at the unit cell boundaries due to densification, potentially causing the soil to yield earlier

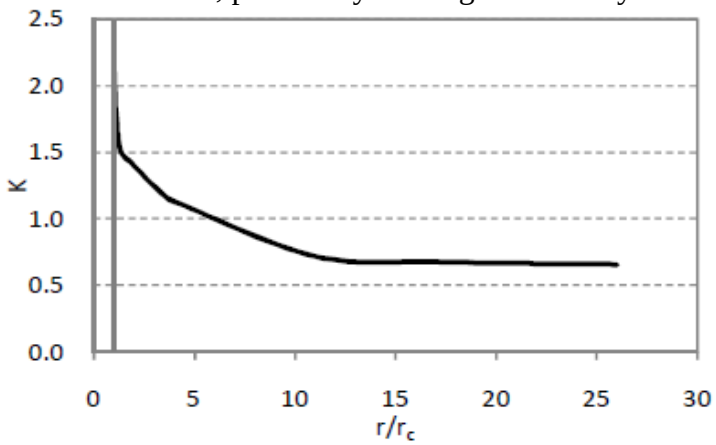

Figure 9: The lateral stress coefficient values versus distance from column centre (adapted from Shien, 2013)

H. Elshazly et al. (2005) pointed out that due to displacements that take place during the stone column construction, there is a significant rise in K_0 value. As well as the lateral earth pressure values are within the range of 1.0 to 1.5 of K_0 with an average of 1.2, and the post-installation values for K^* are fit between the initial value K_0 and the ultimate one K_p, which agrees with (Watts et al., 2000). Table 1 lists various studies versus the K^* value.

Table 1: Estimated (K) values in various studies (a few are adapted from H. Elshazly et al., 2005 & Camelo,2016)*

Reference	Post-installation lateral earth pressure coefficient K^*
H. A. Elshazly et al. (2006)	Between 1.1 and 2.5, with an average of 1.5
Pitt et al. (2003)	Between 0.4 and 2.2, with an average of 1.2
Watts et al. (2000), Goughnour and Bayuk (1979)	Between K_0 and K_p
Priebe (1995)	1.0
Goughnour (1983), Baumann and Bauer (1974)	Between K_0 and $1/K_0$
H. A. Elshazly et al. (2005)	Between 1.0 and 1.5, with an average of 1.2
Kirsch (2006)	Between 1 and 1.7 of K_0
Castro and Karstunen (2010)	1.4 K_0
Lima (2012)	1.39
Carvajal et al. (2013)	Between 1.5 and 2 of K_0
Camelo (2016)	2.3 K_0
Shien (2013)	3.2 K_0

4. Constitutive Modelling

The final load carrying capacity of the geostructure must be evaluated to define its performance (Guéguin et al., 2015). To describe soil functionality, the elasto-plastic response, and the mode of failure, a variety of constitutive models can be used. The soil performance before, during, and after the construction of stone columns can be simulated using these models. Some of the techniques for modelling stone columns include the following:

4.1. Elasto-plastic models

The elasto-plastic model is a sophisticated model that accurately captures the non-linear behaviour and dilatancy of soils observed in laboratory tests. This model incorporates a yield criterion, an associated flow rule, and a work-hardening law, all of which can be calibrated using experimental data obtained from laboratory tests (Guo & Li, 2008).

Typically, the elastic part of the perfectly plastic models is based on Hook´s law, while the plastic one contributes to the conical yield surface (Kok et al., 2009). Uniaxially loaded bar is used to clarify the elastic perfectly plastic response (plastic yielding, hardening, and softening). In Figure 10, part AB represents the elastic response and is governed by Young's modulus E, and the relation of stress-strain is still constant until σ_y (yield stress). Any deformation after point B is exhibit perfectly plastic behaviour. So, if the bar is loaded at point C, the plastic strain ε_c^p will occur, and the remaining strain is defined as $d\varepsilon_c^p = \varepsilon_c - \varepsilon_B$. The figure illustrates the ideal manner of linear elastic perfectly plastic (Potts & Zdravkovic, 2001).

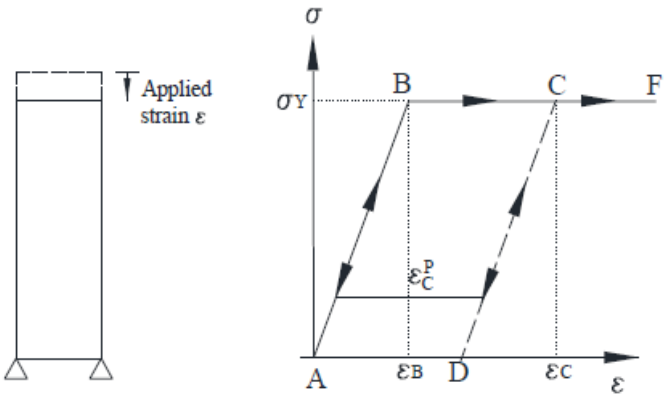

Figure 10: Uniaxial loading, linear elastic perfect plastic behaviour. (adapted from Potts & Zdravkovic.2001)

From a geotechnical point of view, Figure 11-a illustrates the softening behaviour (shear test for sandy soil), while Figure 11-b shows the hardening one (oedometer test for clayey soil).

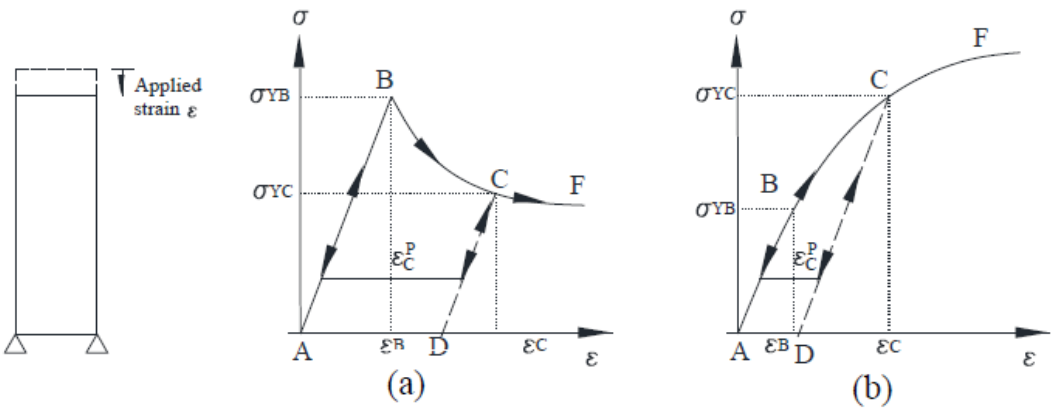

Figure 11: (a) the elasto-plastic for a direct shear test (softening behaviour), and (b) elasto-plastic for oedometer test (hardening soil) (adapted from Potts & Zdravkovic. 2001)

However, elasto-plastic constitutive model includes the following models:

4.1.1. Mohr-Coulomb model

Mohr-coulomb failure criterion can be defined as the following Eq. (3) & Eq. (4). (Camelo, 2016).

$$\tau_f = c' + \sigma'_{nf} tan\varphi' \qquad \textit{Eq. (3)}$$

$$\sigma'_1 - \sigma'_3 = 2c' cos\varphi' + (\sigma'_1 + \sigma'_3) sin\varphi' \qquad \textit{Eq. (4)}$$

$c'$is the effective cohesion, φ' is the effective angle of shearing resistance, τ_f stress shear, σ'_{nf} effective normal stress, $\sigma'_1 = \sigma'_v$ effective vertical stress, and $\sigma'_3 = \sigma'_h$ effective horizontal stress.

The yield/failure surface, can also be expressed using principal stresses as:

$$F(\{\sigma'\}) = \sigma'_1 - \sigma'_3 - 2c' cos\varphi' - (\sigma'_1 + \sigma'_3) sin\varphi' \qquad \textit{Eq. (5)}$$

If

$$\begin{cases} j = \frac{1}{\sqrt{6}} \sqrt{(\sigma'_1 - \sigma'_2)^2 + (\sigma'_2 - \sigma'_3)^2 + (\sigma'_3 - \sigma'_1)^2} \\ p' = \frac{1}{3}(\sigma'_1 + \sigma'_2 + \sigma'_3) \\ \theta = tan^{-1}\left[\frac{1}{\sqrt{3}}\left(2\,\frac{\sigma'_2 - \sigma'_3}{\sigma'_1 - \sigma'_3} - 1\right)\right] \\ g(\theta) = \dfrac{\sin\varphi'}{\cos\theta + \frac{sin\theta x sin\varphi'}{\sqrt{3}}} \end{cases}$$

Eq. (5) can be written as

$$F(\{\sigma'\}) = j - \left(\frac{c'}{tan\varphi'} + p'\right) g(\theta) = 0 \qquad \textit{Eq. (6)}$$

4.1.2. Cam-Clay model

In the isotropic triaxial test, the clay sample compresses in the void-logarithm of mean effective stress (v-ln p´) space, along to the virgin consolidation line. In the unloading stage, the sample will heave/swell along the swelling line. When it is reloaded again, the sample will compress along the same swelling line and then after yield follows the

virgin consolidation line (Camelo, 2016). The following Figure 12 illustrates the virgin consolidation and the swelling line.

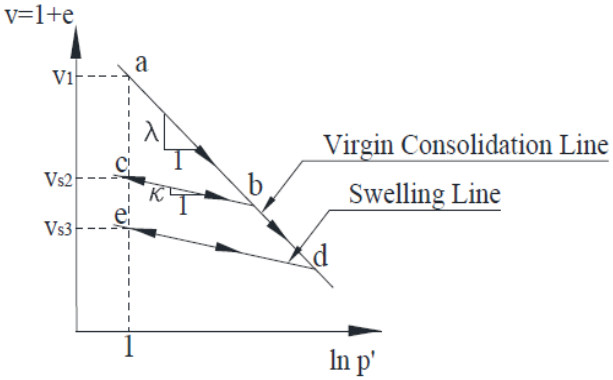

Figure 12:Virgin consolidation and swelling line in isotropic triaxial test.

The equation of virgin consolidation is $v + \lambda(ln\, p') = v_1$ *Eq. (7)*

and for the swelling line is $v + k(ln\, p') = v_s$ *Eq. (8)*

Where the compressibility index λ and the swelling index k are clay soil parameters, and v_s varies according to the swelling line.

The deformations within virgin consolidation are plastic, while for the swelling line is elastic. Furthermore, the yield surface equations for both CAM-Clay and the modified CAM-Clay are:

$$F(\{\sigma'\},\{k\}) = q + M_{p'} ln\left(\frac{p'}{p'_0}\right) = 0 \qquad for\ CAMClay \qquad \textit{Eq. (9)}$$

$$F(\{\sigma'\},\{k\}) = \left(\frac{q}{p'}\right)^2 + M^2\left(1 - \frac{p'_0}{p'}\right) = 0 \qquad for\ modified\ CAM\ Clay \qquad \textit{Eq. (10)}$$

where M is the slope of the critical state line (CSL) in $q - p'$space and it relates to the critical state friction angle.

$q = \sigma'_1 - \sigma'_3$

$p' = \dfrac{\sigma'_1 + 2\sigma'_3}{3}$

p'_0 is the isotropic pre-consolidation stress.

The pre-consolidation pressure p'_0, which is related to plastic volumetric strain $d\varepsilon_v^p$ defines the size of the yield surface by the following equation.

$$\frac{dp'_0}{p'_0} = d\varepsilon_v^p \frac{v}{\lambda - k} \qquad \textit{Eq. (11)}$$

The Figure 13 illustrated the CAM-Clay and modified CAM-Clay yield surfaces

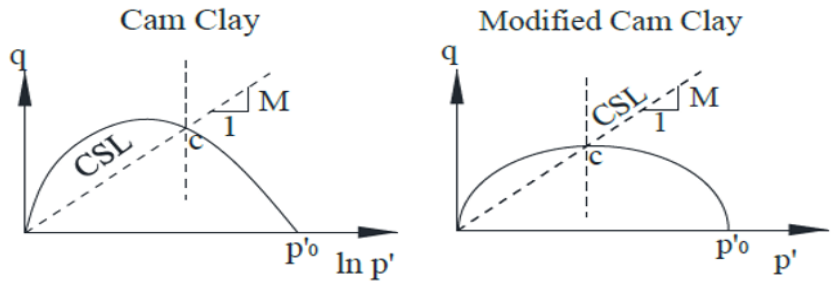

Figure 13: Both CAM Clay model and modified CAM Clay model yield surface (adapted from Potts & Zdravkovic. 2001)

4.1.3. Soft Soil model

According to Neher and Wehnert (2001) the Soft Soil model is based on a modified CAM Clay model with an assumption of a logarithmic relation between the volumetric strain ε_v and the effective stress p´, thus using the modified compression index λ^* instead λ The yielding on virgin isotropic compression can be described as:

$$\varepsilon_v - \varepsilon_{v_0} = \lambda^* ln\left(\frac{p'}{p'_0}\right) \qquad \textit{Eq. (12)}$$

and for isotropic loading and reloading case, where κ^* is the modified swelling index the Eq. (12) can be rewritten as

$$\varepsilon_v^e - \varepsilon_{v_0}^e = \kappa^* ln\left(\frac{p'}{p'_0}\right) \qquad \textit{Eq. (13)}$$

Assuming the behaviour is elastic, so Eq. (13) implies linear stress as the following Eq. (14)

$$E_{ur} = 3(1 - 2\nu_{ur})\frac{p'}{\kappa^*} \qquad \textit{Eq. (14)}$$

where subscript (ur) represents the unloading and reloading situation. The yield function for a triaxial test of SS-model is

$$f = p^{eq} - p_p^{eq} \qquad \textit{Eq. (15)}$$

The p^{eq} is the actual stress state and p_p^{eq} is the equivalent pre-consolidation stress are defined by the following equations (Neher & Wehnert, 2001). See Figure 14.

$$p^{eq} = \frac{q^2}{M^2(p' + c'\,cot\varphi')} + (p' + c'\,cot\varphi') \qquad \textit{Eq. (16)}$$

$$p_p^{eq} = p_{p0}^{eq} exp\left(\frac{\Delta\varepsilon_v^p}{\lambda^* - \kappa^*}\right) \qquad \textit{Eq. (17)}$$

where ε_v^p is volumetric plastic strain

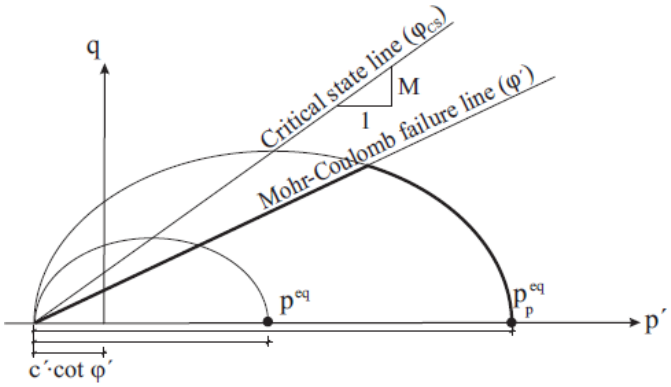

Figure 14: The yield surface in the p'-q plane for the SS-model (adapted from Neher & Wehnert, 2001)

4.2. Elastic-viscoplastic model

This model assumes that the response of the material is influenced by the rate at which it is loaded, exhibiting a rate-dependent or 'viscous' property. The dependence of the undrained shear strength and the pre-consolidation pressures on the loading rate and the size of the yield surface demonstrates this. The basis of viscoplastic straining is the gradual adjustment of particle contacts over time. Creep is a fundamental example of this process; it involves gradually developing plastic strains under constant stress conditions (Kelln et al., 2008). The Elastic-viscoplastic model includes the following constitutive soli models:

4.2.1. Soft Soil-creep model

Buisman (1936) indicated that the consolidation theory cannot fully explain the soft soil settlement. The equation that represents the creep was proposed by Butterfield (1979)

$$\varepsilon^H = \varepsilon_c^H + \mu^* \, ln\left(\frac{\tau_c + t'}{\tau_c}\right) \qquad \textit{Eq. (18)}$$

where ε_c^H is the deformation during consolidation, μ^* is modified creep index, and τ_c is a parameter related to both the test geometry and consolidation. See Figure 15.

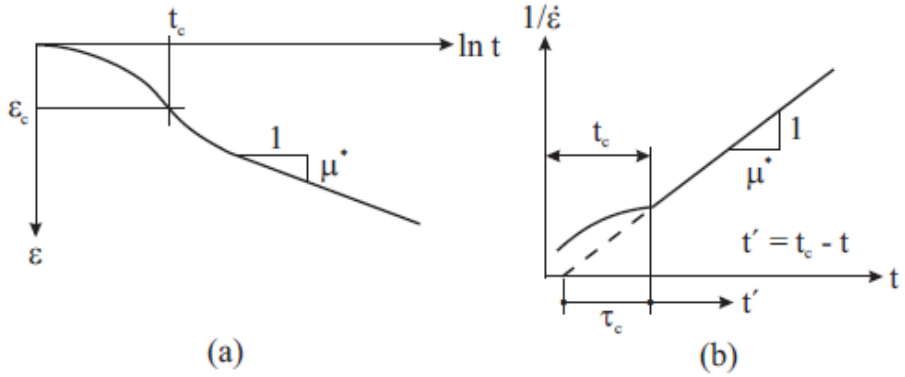

Figure 15: Soft soil consolidation behaviour (a), and creep behaviour (b) (adapted from Neher &Wehnert, 2001)

The strain rate can be computed from the following Eq. (19)

$$\dot{\varepsilon} = \frac{\mu^*}{t' + \tau_c} \quad or \quad \frac{1}{\dot{\varepsilon}} = \frac{t' + \tau_c}{\mu^*} \qquad \textit{Eq. (19)}$$

where the dot refers to differentiation with time. The creep index μ^*can be included in the last equation to get the total volumetric strain

$$\varepsilon_v = \varepsilon_v^e + \varepsilon_v^{cr} = \varepsilon_{vc}^e + \varepsilon_{vc}^{cr} + \varepsilon_{vac}^{cr} = \kappa^* ln\left(\frac{p'}{p_0'}\right) + (\lambda^* - \kappa^*)\ln(\frac{p_{pc}'}{p_{p0}'}) + \mu^* ln\left(\frac{\tau_c + t'}{\tau_c}\right) \qquad \textit{Eq. (20)}$$

ε_v is the total volumetric change when the stress increases from $p_0'$to p' within period $t_c + t'$. However, the volumetric strain contains the elastic part (*e*) and visco-plastic creep part (*cr*). Creep strains are divided into a part that takes place before consolidation (*c*) and other parts after consolidation (*ac*). Eq. (20) can only be applied for constant effective, but when the impact is transitive or continuous, another equation should be applied (Neher & Wehnert, 2001), see Figure 16.

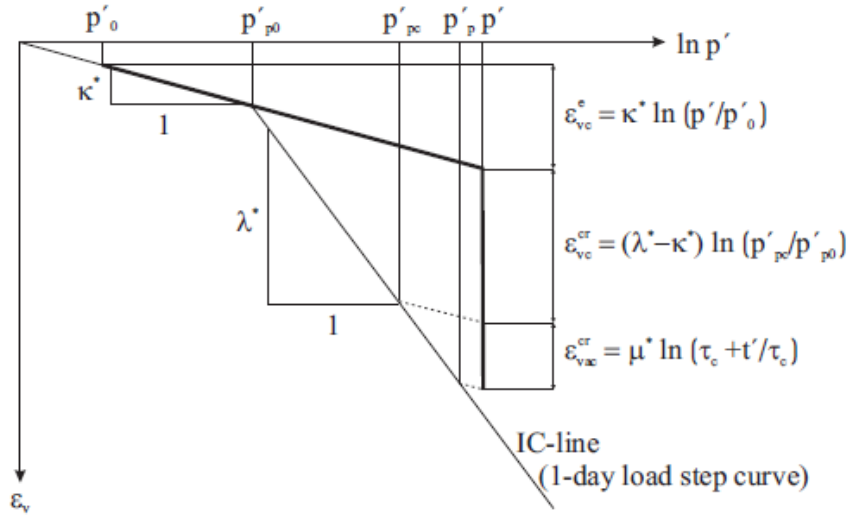

Figure 16: The logarithmic relation between the volumetric strain (inclusion creep) and mean applied stress (adapted from Neher & Wehnert, 2001)

If the inelastic strain is considered as time independent, and the pre-consolidation stress is related to the amount of the accumulated creep strain by time Eq. (20) can be written

$$\varepsilon_v = \varepsilon_v^e + \varepsilon_v^{cr} = \kappa^* ln\left(\frac{p'}{p_0'}\right) + (\lambda^* - \kappa^*) ln\left(\frac{p_{pc}'}{p_{p0}'}\right) \qquad \textit{Eq. (21)}$$

$$p_p' = p_{p_0}' exp\left(\frac{\Delta\varepsilon_v^{cr}}{\lambda^* - \kappa^*}\right),\ so \quad \varepsilon_{vac}^{cr} = (\lambda^* - \kappa^*) ln\left(\frac{p_p'}{p_{pc}'}\right) = \mu^* ln\left(\frac{\tau_c + t'}{\tau_c}\right) \qquad \textit{Eq. (22)}$$

By combining Eq (20) and Eq (21)

$$\varepsilon_{vac}^{cr} = \varepsilon_v^{cr} - \varepsilon_{vc}^{cr} = (\lambda^* - \kappa^*) ln\left(\frac{p_p'}{p_{pc}'}\right) = \mu^* ln\left(\frac{\tau_c + t'}{\tau_c}\right) \qquad \textit{Eq. (23)}$$

Nonetheless, if the applied load is within constant time $t_c + t' = \tau$ (assumed 24 hours), and $p_p' = p'$ so the OCR= 1, Eq. (23) can be written

$$(\lambda^* - \kappa^*) ln\left(\frac{p'}{p_{pc}'}\right) = \mu^* ln\left(\frac{\tau_c + \tau - t_c}{\tau_c}\right) \qquad \textit{Eq. (24)}$$

As $\tau_c - t_c$ is very small, so $\frac{\tau}{\tau_c} = \left(\frac{p'}{p_{pc}'}\right)^{\frac{\lambda^* - \kappa^*}{\mu^*}}$, and the deferential creep formulation will be

$$\dot{\varepsilon}_v = \dot{\varepsilon}_v^e + \dot{\varepsilon}_v^{cr} = \kappa^* \left(\frac{\dot{p}'}{p'}\right) + \frac{\mu^*}{\tau_c + t'} = \kappa^* \left(\frac{\dot{p}'}{p'}\right) + \frac{\mu^*}{\tau_c}\left(\frac{p'_{pc}}{p'_p}\right)^{\frac{\lambda^* - \kappa^*}{\mu^*}} \qquad \textit{Eq. (25)}$$

4.2.2. SCLAY1 model

Many constitutive models can be applied to simulate the anisotropic, plastic behaviour of the soil. The SCLAY1, which was proposed by Wheeler et al. (2003), has advantages over other frameworks, such as simple formulation, realistic prediction of K_0, and the fact that the used parameters can be extracted from laboratory tests. Besides, the model has successfully compared with different tests results from various locations (Karstunen et al., 2005).

Gens and Nova (1993) produced a general framework to combine bonding and destructuration within the elasto-plastic model, where the concept off an intrinsic yield surface is adopted in addition to the actual yield surface for the natural material (i.e., intrinsic yield surface shows the actual size of the yield surface in case there is no bonding). Various similar models were presented, like Kavvadas and Amorosi 2000; Nova et al. 2003, yet none of them considered the anisotropic behaviour, which is a typical for natural soft clays.

SCLAY1S, developed by Koskinen et al. (2002) as an improved model for SCLAY, considers destructuration, bonding, and plastic anisotropy. Figure 17 shows the SCLAY1S yield surface in three dimensions space and triaxial stress space.

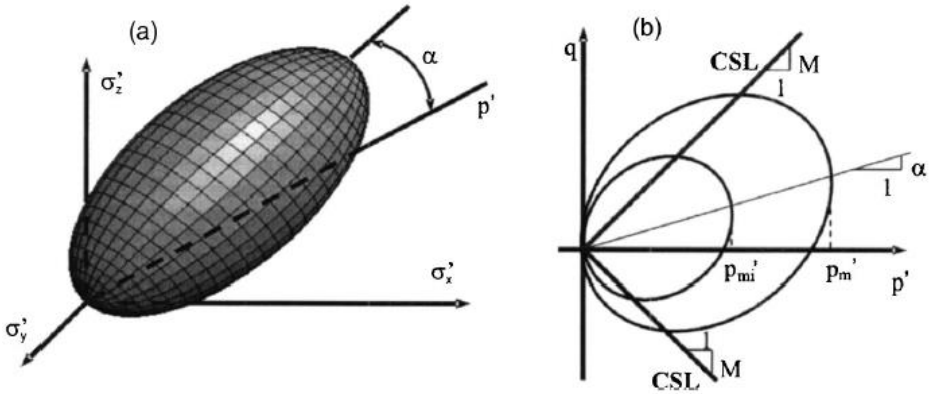

Figure 17: The S-CLAY1S model: (a) three-dimensional space, and (b) triaxial stress space (adapted from Karstunen et al., 2005).

In three-dimensional space the yield surface of S-CLAY1S is defined by the following equation Eq. (26)

$$f = \frac{3}{2}[\{\sigma_d - p'\alpha_d\}^T\{\sigma_d - p'\alpha_d\}] - \left[M^2 - \frac{3}{2}\{\alpha_d\}^T\{\alpha_d\}\right](p'_m - p')p' = 0 \qquad \text{Eq. (26)}$$

where σ_d is the deviatoric stress tensor, p' is the mean effective stress, α_d is the deviatoric fabric tensor, which is a dimensionless second-order tensor to describe the anisotropy, M is the critical state slope value in the stress ratio in triaxial space, and p'_m defines the actual size of the yield surface. Zentar et al. (2004) show how the primary values of deviatoric fabric tensor α_d can be computed.

When both the material and stress state cross the anisotropic and the isotropic plan of material accompany with the stress isotropy plan, the inclination of yield surface in $p' - q$ (q is the deviatoric stress) can be applied instead of α_d(i.e., in-situ situation before load application).

Furthermore, Gens and Nova (1993) described the bonding effect using an intrinsic yield surface. It has the same shape and slope as the real yield surface, while Eq. (27), describes the relation between p'_m and p'_{mi}. Where x is amount of bonding.

$$p'_m = (1 + x)p'_{mi} \qquad \textit{Eq. (27)}$$

The increase in intrinsic yield surface is connected to plastic volume strain incrementation. Eq. (28).

$$dp'_{mi} = \frac{up'_{mi}}{\lambda_i - \kappa} d\varepsilon_v^p \qquad \textit{Eq. (28)}$$

where v is the specific volume, λ_i is the inclination of the normal compression plane in $(lnp' - v)$ space, and κ is the slope of swelling in compression plane. The following equation, Eq. (29). shows the second hardening law, which describes the new angle of the yield surface because of the plastic strain.

$$d\alpha_d = \mu \left(\left[\frac{3\eta}{4} - \alpha_d \right] \langle d\varepsilon_v^p \rangle + \beta \left[\frac{\eta}{3} - \alpha_d \right] d\varepsilon_v^p \right) \qquad \textit{Eq. (29)}$$

$\eta = \sigma_d / p'$ is the tensional equivalent for stress ratio, and $d\varepsilon_v^p$ is the plastic deviatoric incrimination. While μ, β represent the rate at which α_d moves to its target value for both plastic deviatoric and plastic volumetric strains in rotating yield surface (Wheeler et al., 2003).

The third hardening model illustrates the deterioration of bonding. It assumes both the plastic volumetric strain and plastic deviatoric strain. Eq. (30).

$$dx = -ax\left(\left| d\varepsilon_v^p \right| + b \left| d\varepsilon_v^p \right| \right) \qquad \textit{Eq. (30)}$$

The constant (a) defines the absolute rate of deterioration, while the constant (b) describes the comparative effectiveness strains of both plastic deviatoric and plastic volumetric at bond degradation (Koskinen et al., 2000).

4.2.3. Creep-SCLAY1 model

The simplicity of this model is all the parameters can be obtained from triaxial stress space, which can be achieved by subjecting vertically cut, anisotropic sample of soil to oedometer or triaxial test (Sivasithamparam et al., 2015).

Where the stress quantities both the mean effective stress $p' = \frac{\sigma'_a + 2\sigma'_r}{3}$ and the deviator stress $q = \sigma'_a - \sigma'_r$ and the strain quantities both volumetric strain $\varepsilon_\vartheta = \varepsilon_a + 2\varepsilon_r$ and the deviator strain
$\varepsilon_q = 2(\varepsilon_a - \varepsilon_r)/3$ where a and r represent the axial and radial direction respectively.
Both plastic and creep are included in one law

$$\dot{\varepsilon}_\vartheta = \dot{\varepsilon}_\vartheta^e + \dot{\varepsilon}_\vartheta^c \qquad \textit{Eq. (31)}$$

$$\dot{\varepsilon}_q = \dot{\varepsilon}_q^e + \dot{\varepsilon}_q^c \qquad \textit{Eq. (32)}$$

where the dot refers to differentiation with time, e for elastic part and c for creep part. The base of this model is there is no pure elastic domain, where the following equations illustrates the isotropic and deviatoric elastic part

$$\dot{\varepsilon}_\vartheta^e = \dot{p}'/K \qquad \textit{Eq. (33)}$$

$$\dot{\varepsilon}_\vartheta^e = \dot{q}/3G \qquad \textit{Eq. (34)}$$

Where $K = p'/\kappa^*$is the bulk modulus, $G = 3p'/2\kappa^* \left(\frac{1-2\upsilon'}{1+\upsilon'}\right)$ is elastic shear modulus, κ^* is modified swilling index, and υ' is Poisson's ratio.
The outer ellipse is the boundaries between small and large strains (see Figure 18) where volumetric creep strain defines the ellipse size according to the following hardening law Eq. (35).

$$p' = p'_{p0}\, exp\left(\frac{\varepsilon_\vartheta^c}{\lambda^* - \kappa^*}\right) \qquad \textit{Eq. (35)}$$

λ^* is modified compression index, and the isotropic preconsolidation pressure p'_{p0}

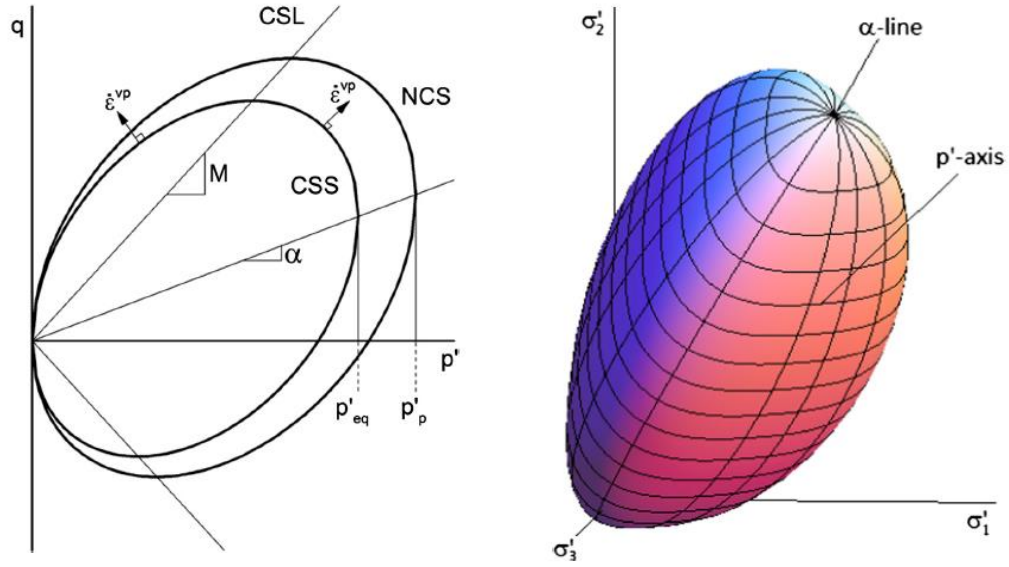

Figure 18: Current state surface (CSS) and Normal consolidate surface (NCS) in Creep-SCLAY1S model to the left, and the Creep-SCLAY1 in general stress space to the right (adapted from Sivasithamparam et al., 2015)

The inner ellipse represents the Current state surface, while p'_{eq} the equivalent mean stress can be defined by the following equation 36.

$$p'_{eq} = p' + \frac{(q-\alpha p')^2}{(M^2(\Theta)-\alpha^2)p'} \qquad \textit{Eq. (36)}$$

where α is a scalar quantity that employed to describe the normal consolidation surface and current stress surface, and $M(\theta)$ is dependent load angle stress ratio at critical state. By applying the concept of a constant rate of visco-plastic multiplier, the creep can be calculated by the following equation 37

$$\dot{\Lambda} = \frac{\mu^*}{\tau}\left(\frac{p'_{eq}}{p'_p}\right)^\beta \left(\frac{(M^2(\theta)-\alpha^2_{K_0^{NC}})}{(M^2(\theta)-\eta^2_{K_0^{NC}})}\right) \qquad \textit{Eq. (37)}$$

where $\eta^2_{K_0^{NC}} = \frac{3(1-K_0^{NC})}{(1+2K_0^{NC})}$, while this part of equation $\left(\frac{(M^2(\theta)-\alpha^2_{K_0^{NC}})}{(M^2(\theta)-\eta^2_{K_0^{NC}})}\right)$ to ensure the inclusion of oedometer test, $\alpha_{K_0^{NC}}$ is the ellipse inclination in normally consolidate state, μ^* is the modified creep index, and τ is time reference and usually is equal to 24 hours. For a standard oedometer $\beta = \frac{\lambda^*-\kappa^*}{\eta^*}$, $\eta^* = \frac{C_\alpha}{ln10(1+e_0}$

To conclude the changes of the normal consolidation surface orientation with creep straining, Creep-SCLAY1 model employs rotational hardening law that allows the evolution of anisotropy simulation. Equation 38 shows the rotational hardening law

$$d_\alpha = \omega\left(\left[\frac{3\eta}{4} - \alpha\right]\langle d\varepsilon^c_\vartheta\rangle + \omega_d\left[\frac{\eta}{3} - \alpha\right]|d\varepsilon^c_d|\right) \qquad \textit{Eq. (38)}$$

where ω_d a soil constant that lies between $\frac{\eta}{3}$ and $\frac{3\eta}{4}$ and defines the relative effectiveness of creep shear strains and volumetric strains, ω defines the absolute rate of yield surface rotation towards the value of α, while $\langle d\varepsilon^c_\vartheta\rangle = d\varepsilon^c_\vartheta$ if $d\varepsilon^c_\vartheta > 0$ and $\langle d\varepsilon^c_\vartheta\rangle = 0$ if $d\varepsilon^c_\vartheta < 0$

As the Creep-SCLAY1 model assumes flow-rule association so the creep strain rate calculates as the following equation 39

$$\dot{\epsilon}_\vartheta = \dot{\Lambda}\frac{\partial p'_{eq}}{\partial p'} \text{ and } \dot{\epsilon}_q = \dot{\Lambda}\frac{\partial p'_{eq}}{\partial q} \qquad \textit{Eq. (39)}$$

M is a function for load angle θ is calculated as Eq. 40.

$$M(\theta) = M_c\left(\frac{2m^4}{1+m^4+(1-m^4)sin3\theta_\alpha}\right)^{0,25} \qquad \textit{Eq. (40)}$$

m = M_e/M_c where M_c is the value of M in compression when $\theta = -30^o$

M_e is the value of M in extension when $\theta = -30^o$

while the modified load angle θ_α that corresponds to α line is calculated as

$$sin3\theta_\alpha = -\left[\frac{3\sqrt{3}(J_3)_\alpha}{2\,(J_2)^{3/2}_\alpha}\right] \qquad \textit{Eq. (41)}$$

where $(J_2)_\alpha$ and $(J_3)_\alpha$ are the second and third invariants of the modified stress deviator $q - \alpha p'$ (Sivasithamparam et al., 2015).

5. Stone column design methods

Installing stone columns essentially speeds the consolidation and increases the bearing capacity of the soft soil. By reducing the void ratio in the effect zone and releasing excess pore water pressure, the stone columns can improve soft soil characteristics (Jakati et al., 2019). However, settlement behaviour tends to gover the stone column design. Whereas most analytical design techniques offer a direct prediction of a settlement improvement factor (n), which is defined as the ratio of untreated ground settlement (s_0) divided by the settlement of the reinforced ground by granular columns (s_t) at a given time t.

$$n = s_0/s_t \qquad \textit{Eq. (42)}$$

From Eq. (31), the expected improved settlement can be calculated

$$s_t = s_0/n \qquad \textit{Eq. (43)}$$

For a large area, the untreated soil settlement factor can be extracted from elastic theory Eq. (33), where P_a is the applied pressure, H is the thickness of the treated earth layer, and E_{oed} is the oedometric soil modulus (Sexton et al., 2013).

$$s_0 = P_a.H/E_{oed} \qquad \textit{Eq. (44)}$$

Generally, for the analytical design method, the factor (n) is related to the area replacement ratio (ARR=A_c/A). Moreover, additional significant factors are incorporated into analytical formulations, including the modular ratio, load level, installation effects, and the friction and dilatancy angles of the column material (Sexton et al., 2013).

Greenwood (1970) presented the empirical and analytical formulas for determining the capacity of individual stone columns. This calculation method utilizes passive horizontal pressure on the soil and assumes the presence of a bulging stone column. Furthermore, Vesic (1972) was the first to depict and analyse the bulging mechanism. Leveraging cavity expansion theory, Vesic could ascertain the soil stresses around the stone column. Mecsi (2013) later elaborated on the principles and application of cavity theory in addressing recent geotechnical challenges.

Madhav and Vitkar (1978) introduced the initial theoretical method to calculating the bearing capacity of a single column. Conversely, Priebe (1995) focused on predicting the capacity of groups of stone columns. Priebe's methodology involved developing a general shear-failure model and assuming the complement lengths for the foundation (i.e., the area of load distribution on soil and stone column). It was presumed that the shear angle and cohesion value of the original soil equated to those of the foundation.

Hu (1995) and Shahu and Reddy (2011) emphasized that the predominant failure pattern for stone column-reinforced ground is the shear failure. However, Stuedlein and Holtz (2013) highlighted that the existing analytical methods do not encompass all scenarios, including settlement-based ones.

Two main approaches are applied to design the stone column:

5.1. Single column approach

This way assumes that the stone column will behave and collapse independently of the other columns. Accordingly, many methods treat the column as a singular pile.

However, it is uncommon to apply granular columns individually. Thus, calculating the capacity of the column group by multiplying the capacity of an individual column by the total number of columns is considered conservative. (Sondermann et al., 2016). Figure 19 illustrates the potential failure mode of a single column.

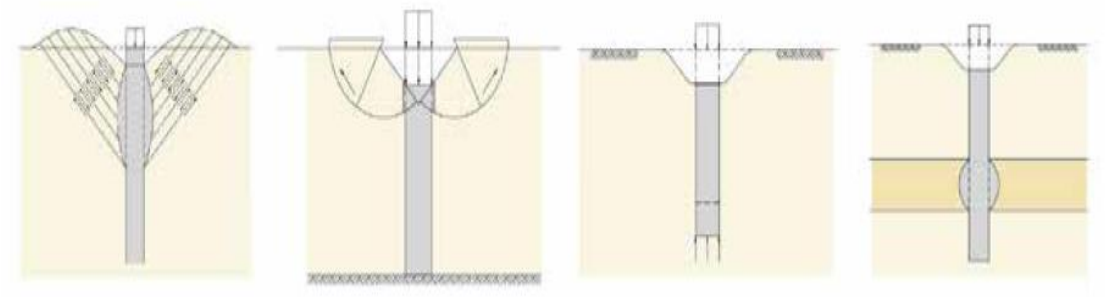

Figure 19: The possible failure modes of single stone column" bulging of long column, shearing failure of short column, sinking of floating column, and bulging in deep soft clay from left to right (adapted from Kirsch and Kirsch. 2010)

5.2. Group of columns approach

Typically, a substantial quantity of stone columns is utilized as the required improvement will be over a spread ground area. While the performance of a group of columns differs significantly from that of a single column, the behaviour also varies depending on whether there is a rigid foundation or a flexible load transfer platform in place (Sondermann et al., 2016). Wood et al. (2000) highlighted the importance of the area replacement ratio, and distinctions between single columns and groups regarding load distribution and interaction. Figure 20 shows the possible failure mechanism for a group of columns.

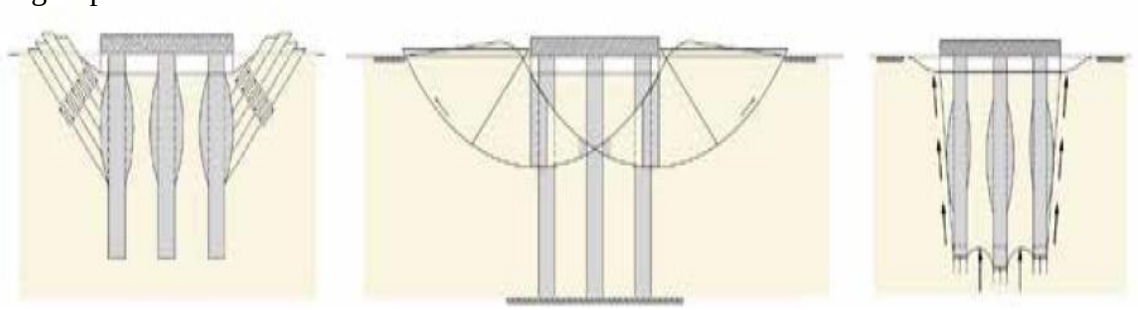

Figure 20: The different failure modes for group of stone columns (adapted from Kirsch and Kirsch. 2010)

Babu et al. (2012) identified five primary numerical methodologies for the design of stone columns. They are as follows: (i) The axisymmetric design, which is a "unit cell" made up of just one column and the surrounding affected soil (Area replacement ratio) (Balaam & Booker, 1981); (ii) The plane strain model, in which the columns are modelled as stone trenches, which are frequently applied with long period loads, like

embankments (Van Impe & De Beer, 1983); (iii) The axial symmetry technique, where stone rings are modelled in place of cylindrical columns to simulate its behavior under circular loads, like tanks (Elshazly et al., 2008); (iv) The homogenization technique, which can be used to model the improved homogeneous soil with stone columns using the composite soil parameters (Jellali et al., 2005) and (Abdelkrim & Buhan, 2007); (v) FEM model (3D), which counts as a complex simulation for stone column (Weber at al., 2008)

The following is a detailed discussion of some of the applied design methods:

5.3. Unit cell (UC) method

The base of the unit cell concept is the idea of a large grid with uniformly spaced columns under a constant load. Since all the columns will behave similarly, as a result an investigation of only one column and its contributed soil area will be sufficient (Ng & Tan, 2014). Because of the symmetry conditions, it is supposed that there are no shear stresses around the perimeter of the unit cell. Columns close to the boundary of the loaded area boundaries are exempt from the unit cell method, as the applied stress will be minimal (i.e., only vertical displacements and water seepage are applied) (Sexton et al., 2013; Castro, 2017). However, Barksdale and Bachus (1983) pointed out that in the unit cell model, the columns experienced shearing force, particularly at the edge of the improved area. See Figure 21.

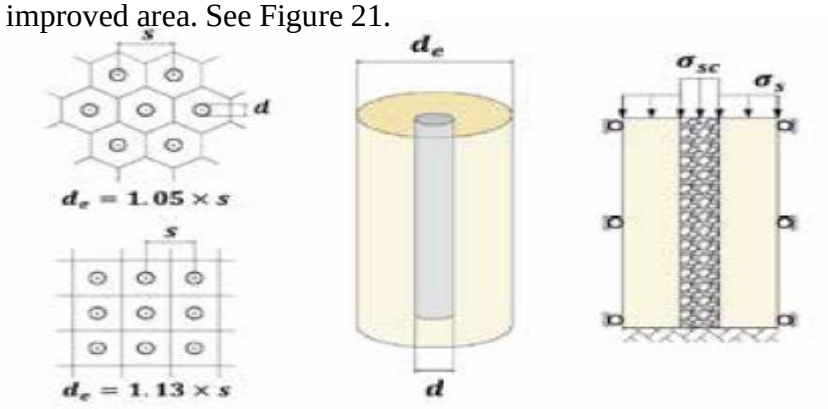

Figure 21: Unit cell design method. (adapted from Sondermann et al., 2016)

The unit cell method is based on the idea of strain compatibility, which states that vertical strains in any horizontal plane are equivalent (i.e., the equilibrium method). This indicates that the vertical deformation in the soil and column at the top of the cell is the same. See Eq. (34). These assumptions make sense for columns with uniform loading in a large grid (Sondermann et al., 2016; Sexton et al., 2013). Both the settlement of untreated ground and the settlement after ground improvement can be calculated as Eq. (32,33).

$$P_a A = \sigma_c A_c + \sigma_s (A - A_c) \qquad \textit{Eq. (45)}$$

Where P_a is the applied load, Ac, A are column and effective area respectively, and σ_c, σ_s are the stresses in column and soil respectively.

Castro (2017) indicated that the ratio of the loaded area and the thickness of the soft soil layer B/H should be large enough, so that the oedometer condition is still applicable. However, in reality, the applied loads spread according to depth (i.e., in a

nearly trapezoidal form), see Figure 22. Because the unit cell model does not consider the load distribution with depth, its conclusions are therefore conservative.

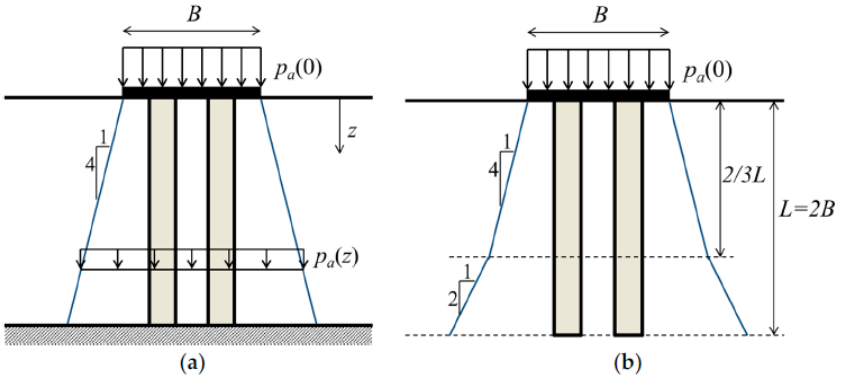

Figure 22: Soil stress distribution under foundation (a) for end bearing column and (b) for floating one (adapted from Castro, 2017)

5.4. Homogenization method

Homogenization is a prevalent technique for analysing the enhanced shear strength of treated ground. This method assumes uniform shear strength parameters within the improved ground. The composite parameters, which represent the equivalent shear strength characteristics of the treated ground, are determined through the area replacement ratio (ARR) or, more practically, a stress concentration ratio (SCR). See Eq. (44). Because this method calculates a weighted average of inputs that excludes the influence of column installation (such as densification and column stiffness), it is considered conservative (Sondermann et al., 2016; Castro, 2017).

$$E_m = E_s(1 - a_r) + E_c a_r \qquad \textit{Eq. (46)}$$

Where m is the equivalent for homogeneous soil, a_r is area replacement ratio, and E_s, E_c is Young's modulus for soil and column respectively.

Ng and Tan (2015) proposed a novel simplified design model, based on a semi-empirical homogenization model, to predict both the settlement and consolidation time of stone columns. The Equivalent Column Method (ECM) principle relies on the elastic perfectly plastic theory, making it superior to previous methods as it accounts for plastic strain resulting from pressure increase. However, this approach overlooks changes in permeability and consolidation coefficient during consolidation or loading.

Guéguin et al. (2015) introduced an integral yield design homogenization method for computing the strength characteristics of improved soil. This method offers two key advantages: it requires few parameters and maintains the constraints on the upper and lower bounds of the obtained domains. The differences between these bounds did not exceed 16%, indicating its accuracy as a method.

5.5. Plane Strain (PS) method

Various stone-column design methodologies utilize the stress concentration ratio (SCR) to calculate equivalent shear strength parameters. The SCR typically rises with soil consolidation (Barksdale & Bachus, 1983). Factors such as the length of the columns, the angle of shearing, and the ratio of Young's modulus (E_{sc}/E_s), along with the area

replacement ratio (ARR), collectively influence the SCR (Sondermann et al., 2016). While the unit cell model is employed for individual columns, the plan strain method is applied for groups of columns, such as column trenches (Gaber et al., 2018b).

Van Impe and De Beer (1983) proposed an analytical method that assumed the soil and columns have similar drainage properties, while the group of columns is simulated as a trench of gravel that has the same ARR. See Figure 23. According to Castro (2017), this method is reasonable as it counts both the same properties for soil and column and the same ARR. However, it has two drawbacks: the ARR is small, so that the trench will be slender, and the confining properties of the stone column are not similar to those of trench one.

Figure 23: Column confining and seepage pattern vs trench confining pattern (adapted from Castr,2017)

Moreover, Tan et al. (2008) proposed two ways to define an equivalent for stone trench and soil properties, but they are not practical. The equation used to define the trench and soil elastic modulus is only applied to elastic behaviour (Castro, 2017).

However, Gaber et al. (2018b) observed a slightly higher SCR in unit cell design compared to plan strain design. In the unit cell design method, the SCR ranged between 2.48 and 3.14, whereas in the plan strain method, it ranged between 1.76 and 2.93. Moreover, the settlement improvement factor (SIF) was more significant in plan strain design than in unit cell design, possibly due to the inclusion of friction and interaction between the columns and the soil in the plan strain model (Gaber et al., 2018a).

Furthermore, regardless of the modelling technique employed, increasing the diameter of the columns, decreasing the spacing between them, and boosting the friction angle all lead to decreased settlement and enhanced pore pressure dissipation (Gaber et al., 2018a).

5.6. Finite Element Method (FEM)

Research using finite element models is usually more comprehensive, but it also requires a good understanding of the modelling techniques. While the application of ground improvement techniques, such as stone columns, has increased because of worries about the environment and the growing projects constructed on soft soils, the analysis of stone column modelling seems like an interesting and useful advancement (Castro, 2017).

Many simplifications that applied in semi-empirical or analytical methods can be overcome using finite element (FE) and finite difference modelling tools. Time effects, different load scenarios, differences in soil properties, and variations in geometry across the issue space can all be considered with modern FE models (Sondermann et al., 2016). Balaam developed a model for an enhanced soft clay that allows measuring the influence of the stone columns on deformation. Additionally, Balaam and Booker (1981) conducted many studies on the deformation behaviour of columns group that support rigid slabs. Mitchell and Huber (1985) compared their model of axisymmetric finite-element of group of columns with the field results, while Kirsch and Sondermann (2003) produced a 3D model and compared the results with a practical study. Kirsch also applied the FE model to examine the installation impact and settlement response of the column group (Sondermann et al., 2016).

Initially, unit cell modelling was employed in FE methods, but Wehr and Herle utilized the Plane Strain (PS) model to predict ground deformation. Weber stratified it to define equivalents for certain soil parameters, like permeability. Tan introduced two simple design methods for modelling granular columns without altering the permeability. Recently, numerous stone column models have integrated 3D modelling to study arching, stress concentration, and soil-column interaction. Primarily, it is important to assess the influence of permeability on soil consolidation in terms of pore pressure and deformation changes (Sondermann et al., 2016).

Despite its efficiency, the FE method involves simplifications that must be accounted for during modelling. For instance, accurately predicting installation effects, such as densification of silt and sands or initial loss and subsequent gain of shear strength in soft clays, poses significant challenges. Another example is the impact of erecting a working platform on soft clays, which can shift or disturb the clay and alter the initial strength profile of the in-situ ground. Thus, calibrations are essential since simplifications are inherent even in the most intricate models (Sondermann et al., 2016).

6. Case Study

The design of foundations is a major concern in regions with very soft soil conditions. This soil type often exhibits low bearing capacity, excessive settlement, and potential structural instability (Borges et al., 2009). However, amidst these challenges, stone columns offer a promising solution. When used for stability improvement, stone columns can effectively reduce and accelerate settlements (Borges et al., 2009), demonstrating their potential to address the issues posed by soft soil conditions.

While stone columns can be effective in improving soft soils, their use in very soft clay poses several challenges. The properties of soft soil, such as collapsing boreholes, excessive soil displacement, and clogging of column materials, can hinder the construction process. Moreover, the tendency of the clay to deform and move over time can cause the stone column to bulge, reducing its load-bearing capacity and compressibility. Furthermore, the long-term performance of stone columns in soft clay is uncertain, which can lead to differential settlement of the foundation despite of the applied improvement method. Additionally, the lack of visibility into the installation process and gravel behaviour within the soft soil adds to the complexity of the process.

This project launches a comprehensive study and exploration into the suitability of a stone column as a ground improvement method for extremely soft soil (Swedish soil). Various constitutive models (Soft Soil (SS), Soft Soil-creep (SSC), and Creep-SCLAY1S are applied to study the problem using the Unit cell (UC) method in Plaxis 2D. The aim is to develop Priebe-type diagrams for each soil model.

6.1. Numerical Model

By applying the UC model for stone column analysing, the numerical model study will be limited to the final settlement and consolidation, without considering the stability. Namely, UC model is not suitable for determining the stability of the reinforced ground (Castro, 2017). See Table 2.

Table 2: The suitability of different geometrical models for various types of stone column studies as an embankment foundation (adapted from Castro. 2017)

Geometrical Model	**Final Settlement**	**Consolidation**	**Stability**
Unit Cell (UC)	***	***	x
Plane Strain (PS) (gravel trench)	**	**	**
Homogenization	**	*	*
3D Slice	***	***	***

**** very suitable, ** moderate suitable, * slightly suitable, x- not suitable*

The study utilizes the finite element software Plaxis V22 / Ultimate (15 nodded triangular, fine mesh, and axisymmetric) to create a numerical model of a standard

scenario to obtain the diagrams. The model consisted of a uniform grid of end-bearing columns under a fill, with each column and the soil around it represented as a unit cell.

As all columns react similarly to loading, the same conditions are assumed to be applied. Additionally, rigid, frictionless, and shear-free boundaries were used except at the top boundary where the embankment is located.

The model will investigate the impact of replacement ratio A/A_c, and the effective friction angle φ′ of the gravel on the improvement factor for the various models.

6.1.1. Model Parameters

For Creep-SCLAY1S soil inputs, the parameter of Ønsoy clay of 5.5-11m depth layer from Hernvall et al. (n.d.) paper will be used, while the Soft Soil (SS) and Soft Soil-creep (SSC) parameters (λ^*, κ^*, λ^*_i, κ^*_i) will be obtained by matching the $(\varepsilon, \sigma_{yy})$ oedometer test presented the Creep-SCLAY1S with SS, and SSC tests. The values adopted are shown in Table3.

Table 3: Inputs parameters for Creep-SCLAY1S, Soft Soil, and Soft Soil- creep models

Creep-SCLAY1S	**ɣ** kN/m^3	**E_{oed}^{ref}** kN/m^2	**$C_{ref.int}$**	**ψ**	**κ^***	**ν'**	**λ^*_i**	**M_c**	**M_e**	**ω**
	16.6	5000	1	0	0.01	0.2	0.062	1.3	1	10
	ω_d	**ξ_d**	**ξ**	**POP**	**OCR**	**K_0**	**χ_0**	**μ_i^***	**τ**	**α_0**
	0.85	0.35	13	25	1.5	0.58	14	2.6E-03	1	0.5
	k_x (m/d)	**k_y** (m/d)								
	2.7E-03	2.7E-03								
SS	**ɣ**	**$C_{ref.int}$**	**φ'**	**ψ**	**κ^***	**ν'**	**λ^***	**OCR**	**K_0^{NC}**	**K_0**
	16.6	1	32.4º	0	1E-3	0.2	0.021	1.5	0.47	0.58
	k_x(m/d)	**k_y**(m/d)								
	2.7E-03	2.7E-03								
SS-creep	**ɣ**	**$C_{ref.int}$**	**φ'**	**ψ**	**κ^*_i**	**ν'**	**λ^*_i**	**μ_i^***	**OCR**	**K_0^{NC}**
	16.6	1	32.4º	0	1E-3	0.2	0.061	2.6E-03	1.5	0.47
	k_x (m/d)	**k_y** (m/d)	**K_0**							
	2.7E-03	2.7E-03	0.58							

Similarly, the used inputs parameters for the layers representing the embankment and the dry crust layer were extracted from the same study, see table 4.

Table 4: Inputs parameters for dry crust and embankments layers (adapted from Hernvall et al. n.d)

Dry Crust Layer	**ɣ** kN/m^3	**E_{oed}^{ref}** kN/m^2	**ν'**	**$C_{ref.int}$**	**φ'**	**ψ**	**k_x** (m/day)	**k_y** (m/day)
	18	5000	0.25	11	5º	0	0.0008	0.0008
Embankments Layer	**ɣ** kN/m^3	**E_{oed}^{ref}** kN/m^2	**ν'**	**$C_{ref.int}$**	**φ'**	**ψ**	**k_x** (m/day)	**k_y** (m/day)
	19.5	4E+04	0.35	2	45º	0	0	0

The input parameters for the working platform and gravel are illustrated in Table 5.

Table 5: Inputs parameters for stone column and platform

Platform Layer	**ɣ**	**E_{oed}^{ref}**	**ν'**	**$C_{ref.int}$**	**φ´**	**ψ**	**k_x** (m/day)	**k_y** (m/day)
	19	2E+04	0.33	1	35º	0	0	0

Stone column	**ɣ**	**E_{50}^{ref}**	**E_{oed}^{ref}**	**E_{ur}^{ref}**	**ν'**	**C**	**φ´**	**ψ**	**kx=ky** (m/day)
	20	5.5E+04	4.9E+04	1.65E+05	0.3	1	45º-37,5º	φ´-30	86

The soft clay layer is assumed to extend to a depth of 25 metres, with 1 meter thick dry crust layer. The groundwater level is assumed to sit 1.2 metres below the ground surface. The working platform has a thickness of 0.5 meters, and the total height of the embankment is 2 meters, consisting of four layers, each 0.5 metres thick. For each layer, one day for consolidation was defined to simulate the time-dependent construction process. The stone columns, measuring 25 metres in length, penetrate through all soil layers to reach bedrock, rendering them a non-floating type. See Figure 24.

For analysis, the dry crust, embankment, and platform layers will be simulated using the Mohr-Coulomb model, while the stone columns will be modelled using the Hardening Soil model.

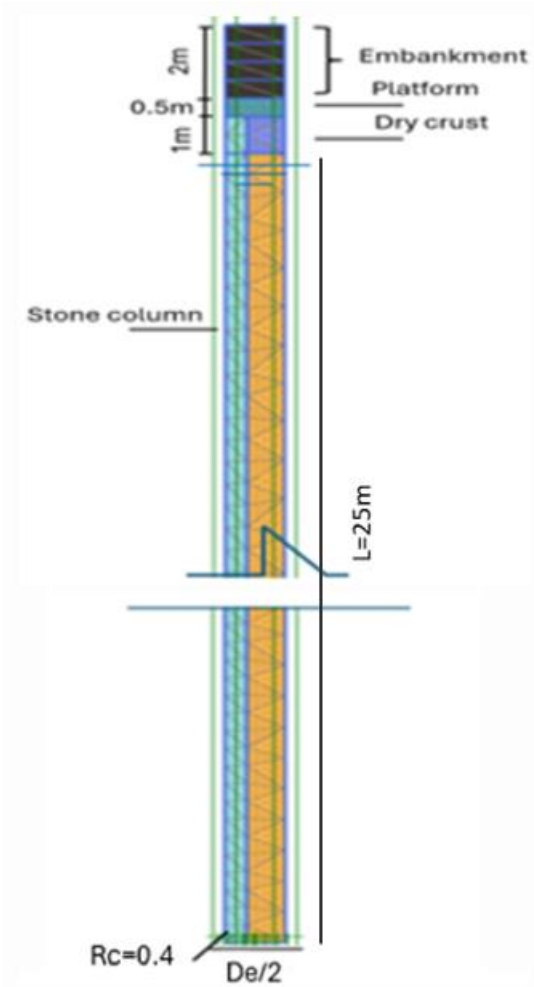

Figure 24: Axisymmetric unit cell Plaxis model, boundary conditions, ground water level, and soil layers thickness.

The diameter of the stone column is assumed as 0.8m, and the chosen column arrangement is a triangular grid pattern. As a result, the diameter of the effective circle (D_e) is calculated to be 1.05 times the spacing between columns (S).

Typically, the distance between columns (S) is 2 to 3 times the diameter. Therefore, the spacing between columns will be between 1.6 to 2.4 metres, and the effective diameter will be between 1.7 to 2.5 metres. This corresponds to an A/A_c ratio ranging from 4.5 to 9. However, for the purposes of this study a narrower range of effective diameters (1.5 to 2.2 metres) and A/A_c ratios (3.1 to 7.6) was applied. See the following Table 6.

Table 6: Stone column spacing, the related effective diameter and area replacement ratio

Spacing (S)	1.3	1.4	1.5	1.6	1.7	1.8	1.9	2	2.1
Effective diameter (D_e)	1.4	1.5	1.6	1.7	1.8	1.9	2	2.1	2.2
Area Replacement ratio (A/A_c)	3.1	3.5	4	4.5	5	5.6	6.2	6.9	7.6

6.1.2. Model Verification

To verify the Creep-SCLAY1S model, the unit cell simulation is compared to the measurements of Berre (2014) considering unreinforced ground, using the same embankment construction schedule, see Table 7. The results show minor discrepancies between the two models. As shown in Figure 25, the small differences can be attributed to the fact that the paper model only considers the parameters of a single clay layer between 5.5 and 11m in depth. In contrast, Berre's model includes four clay layers.

Table 7: Construction stages for verification model (adapted from Berre.2014)

Consolidation Phase		
Phase description	Duration days	Accumulation days
Start	0	20
Fill 0.5	1	21
Wait	1	22
Fill 0.5	1	23
Wait	3	26
Fill 0.5	1	27
Wait	3	30
Fill 0.5	1	31
Wait	2	33
Fill 0.5	1	34
Consolidation	1084	1118

In parallel, the model was with Soft Soil-creep, and its results were compared with those obtained from the Sexton and McCabe (2014) model. The difference between the two models of the compression index parameter was set to 0.0288 in the paper model, similar to the value used in the Sexton and McCabe (2014) model. Figure 26 compares the results obtained from both models in terms of the settlement improvement factor,

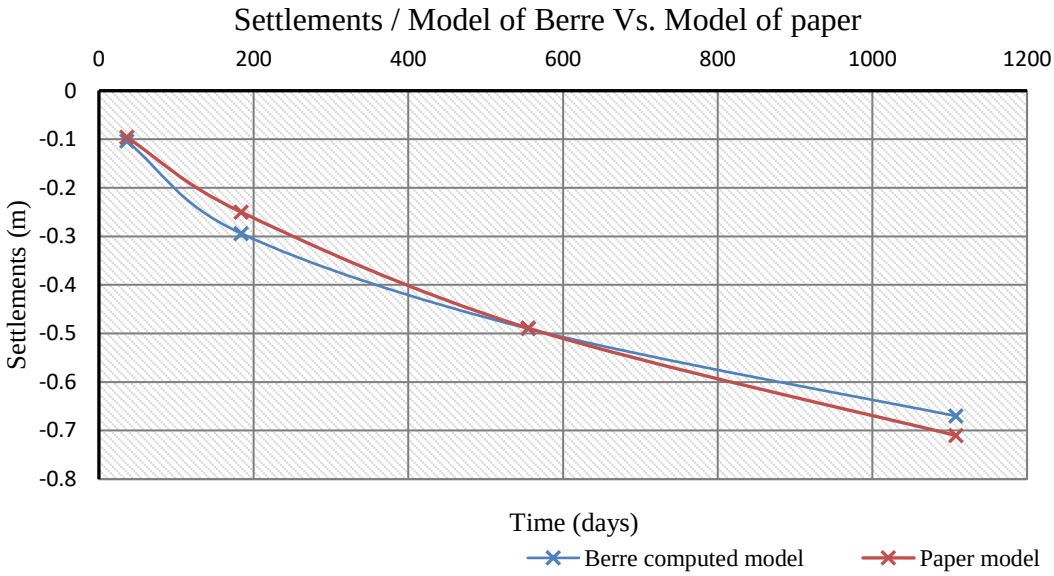

Figure 25: Settlements comparison between the Berre (2014) model and the paper model.

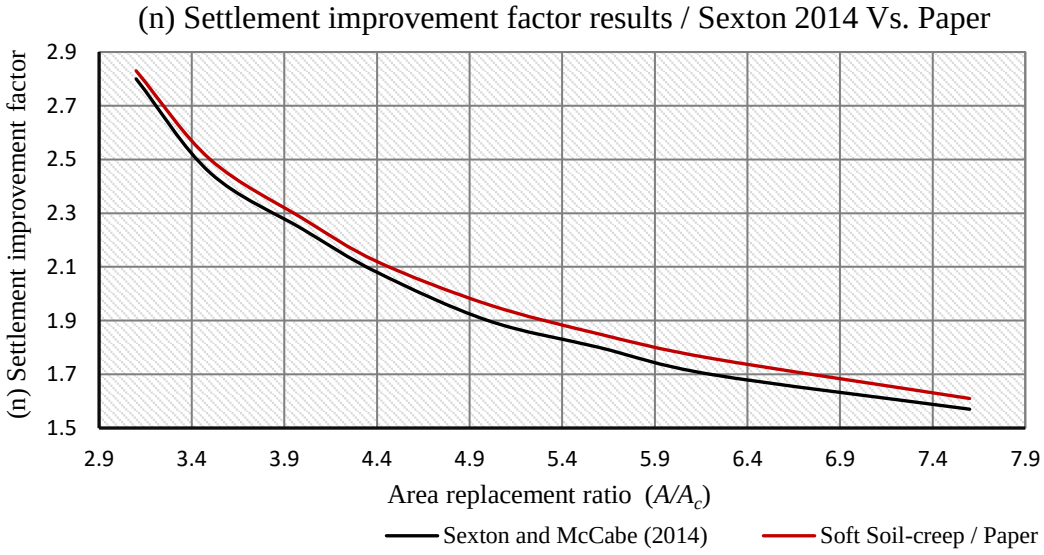

Figure 26: Results comparison of the Sexton and McCabe (2014) model and the paper model considering the creep effect.

The slight difference in the improvement factor (approximately 2%) can be attributed to the differences in the stone column diameter and the E_c/E_s ratio in the two models, in addition to the differences in other soil parameters also contribute to these differences.

6.2. Results and discussion

The numerical model was run with three different constitutive models (Creep-SCLAY1S, Soft Soil, and Soft Soil-creep) to investigate the impact of various A/A_c ratios on the behaviour of the stone column. For each A/A_c value, the settlement improvement factor (n) was calculated by dividing the settlement under untreated conditions by the settlement under treated conditions.

Moreover, the resulting diagrams show the relationship between the effective friction angle of the stone column (φ') and the settlement improvement factor (n) for different periods.

6.2.1. Results of Creep-SCLAY1S model

Diagrams (Figure 27, 28, and 29) illustrate the improvement factor changing with A/A_c ratio changing for 1, 2, and 50 years.

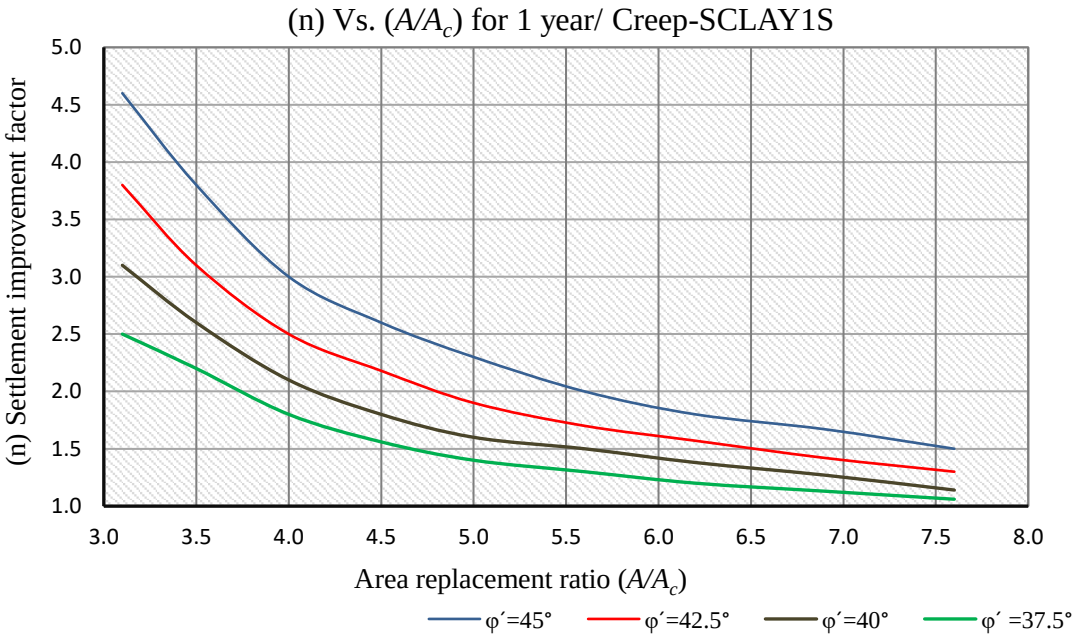

Figure 27:The correlation between the settlement improvement factor (n) and the A/A_c ratio over a one-year time frame with vary effective friction angles of the stone column.

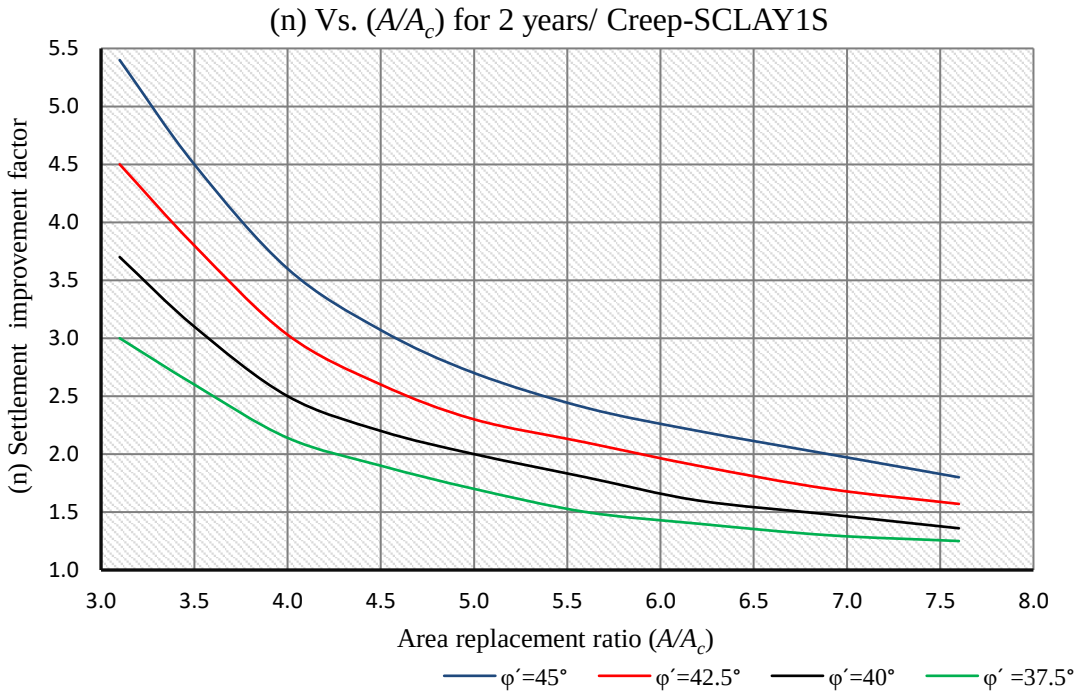

Figure 28: The correlation between the settlement improvement factor (n) and the A/A_c ratio over a two-year time frame with varying effective friction angles of the stone column.

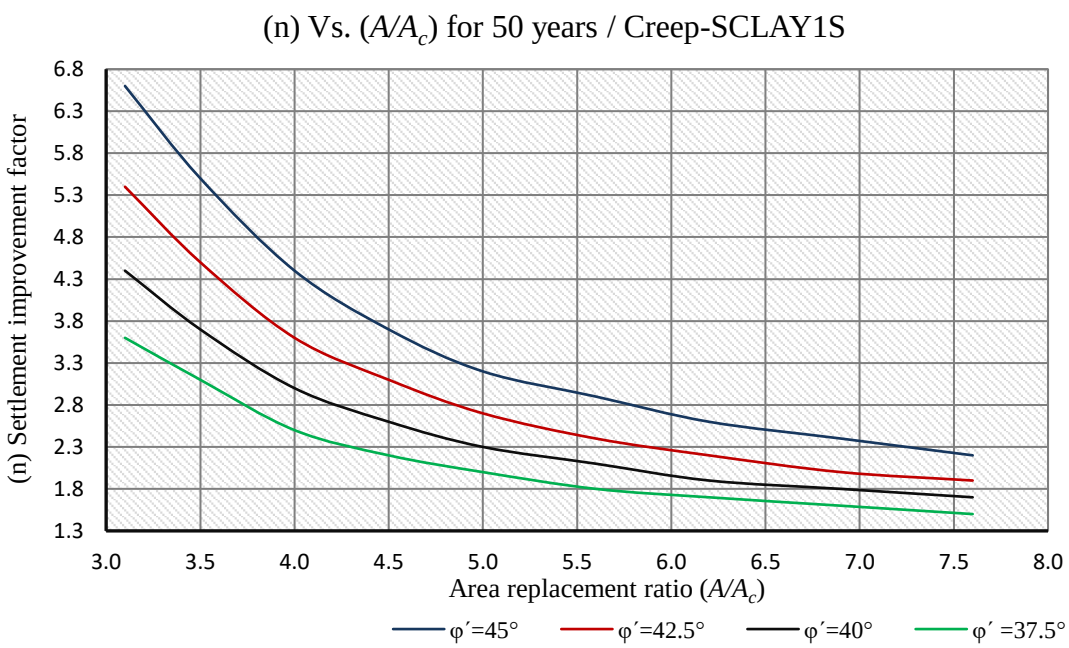

Figure 29: The correlation between the settlement improvement factor (n) and the A/A_c ratio over a fifty-year time frame with varying effective friction angles of the stone column.

Using stone columns in soil improvement is significantly effective, with an 85% reduction in soil settlement when the replacement ratio is 3.1 and the effective friction angle is 45°, compared to Pietraszewska (2011), where the reduction factor of settlement was 81.8%. The difference in the stone column diameter can explain this variation between the two studies.

However, it is essential to note that when the effective friction angle is reduced to 37.5°, the effectiveness of the stone columns decreases to 72%. Similarly, at a replacement ratio of 3.5, the improvement in soil settlement is about 82% for an effective friction angle of 45° but only 67% for an effective friction angle of 37.5°. This highlights the crucial role of the effective friction angle of the stones in the effectiveness of stone columns.

Further increases in the replacement ratio to 5 and 7.6 lead to decreased effectiveness, with improvements in soil settlement dropping to 69% and 54% for an effective friction angle of 45° and to 50% and 34% for an effective friction angle of 37.5°, respectively.

Figure 30 compares the results of the reduction settlement factor obtained by McCabe (2014) using the Creep-SCLAY1S (ANIS & destructuration model) and the paper model, with a 50-year time frame and a stone column effective friction angle of 45º. The comparison shows that the two methods produce varying results, with a 14% to 18% difference when the stone column length (of the paper mode) is 25m and an 5% to 9% difference when the stone column length is 5m equal to the column length in McCabe model. The disparity is attributed to differences in stone column dimensions, such as diameter, ratio of E_c/E_s, and other soil parameters like creep, destructuration, and bonding coefficients. Interestingly, increasing the stone column length from 5m to 25m increases the improvement factor value by about 10% on average, with a value of

6.6, and 2.9 for L_c=25m compared to 4.7, and 2.2 for L_c=5m at a replacement ratio of A/A_c=3.1 and 5.6 respectively.

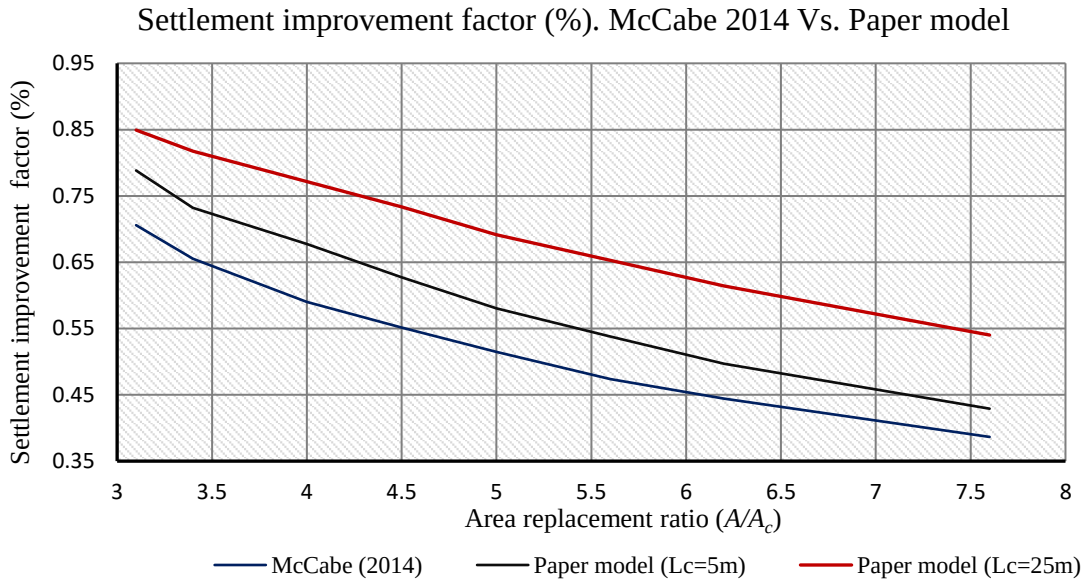

Figure 30: Comparison of settlement improvement factor of McCabe (2014) model and paper model (Creep-SCLAY1S, 50 years, 45º)

Figures 31 and 32 depict the evolution of the improvement factor over time, concerning the A/A_c ratio, for stone columns with effective friction angles of 37.5° and 45°. The results show that the main settlement improvement occurs over approximately twenty years for both effective friction angles, indicating the long-term effectiveness of stone columns.

Interestingly, the settlement reduction in soil treated with stone columns featuring a 45° effective friction angle was more pronounced, indicating a longer-term benefit to using stone columns with higher effective friction angles. This suggests that the use of stone columns can lead to significant and lasting improvements in soil stability.

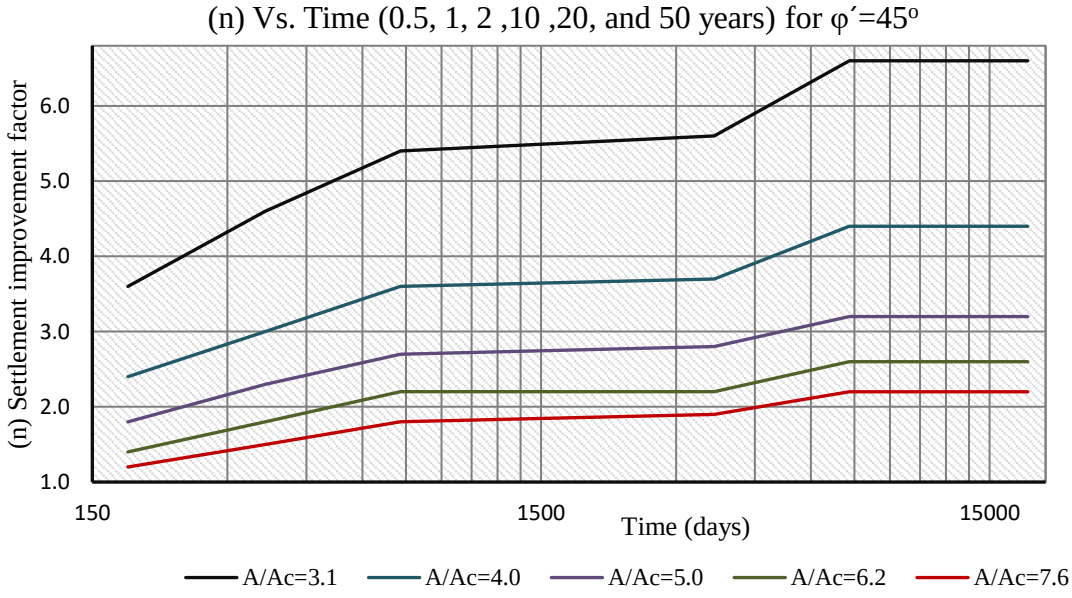

Figure 31: The correlation between the settlement improvement factor (n) and the A/A_c ratio analysed for different time frames at an effective friction angle of 45º.

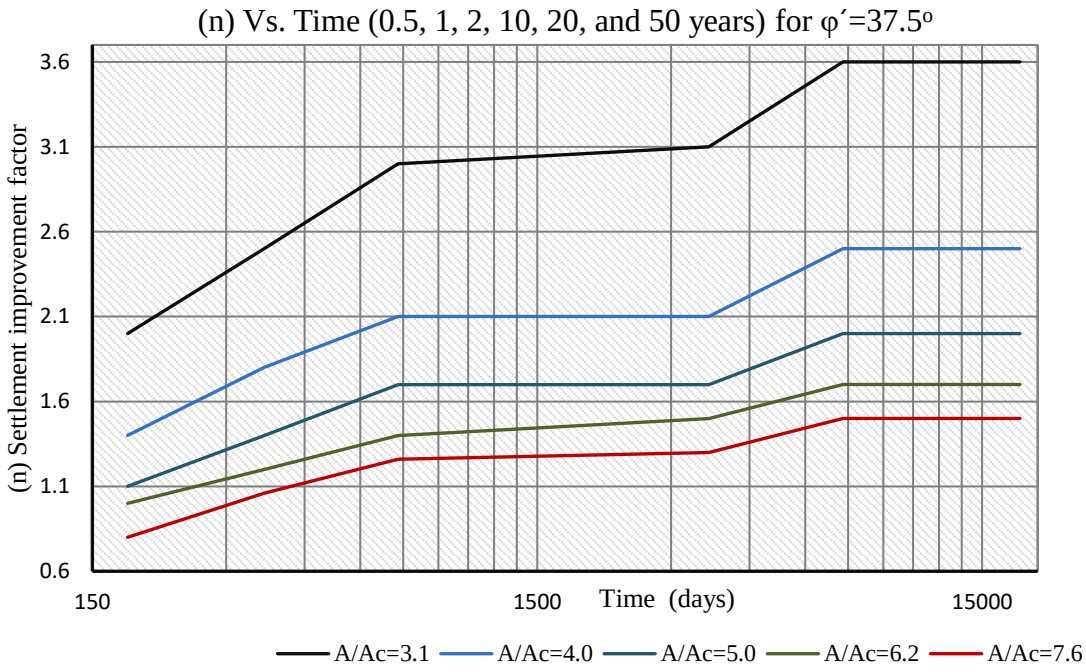

Figure 32: The correlation between the settlement improvement factor (n) and the A/A_c ratio analysed for different time frames at an effective friction angle of 37.5º.

Figure 33 shows the impact of stone column application on the time for settlement. The study reveals that using stone columns can significantly accelerate the consolidation process and reduce the required time for settlement. Specifically, the results indicate that by day 1000, the treated soil with a replacement ratio of 3.5 and 7.6 had settled to approximately 66% and 64% of their total settlements, respectively, while the untreated soil had reached only 58%.

Additionally, the treated soil with replacement ratios of 3.5 and 7.6 achieved half of its total settlement, about 76% and 71% faster than untreated soil.

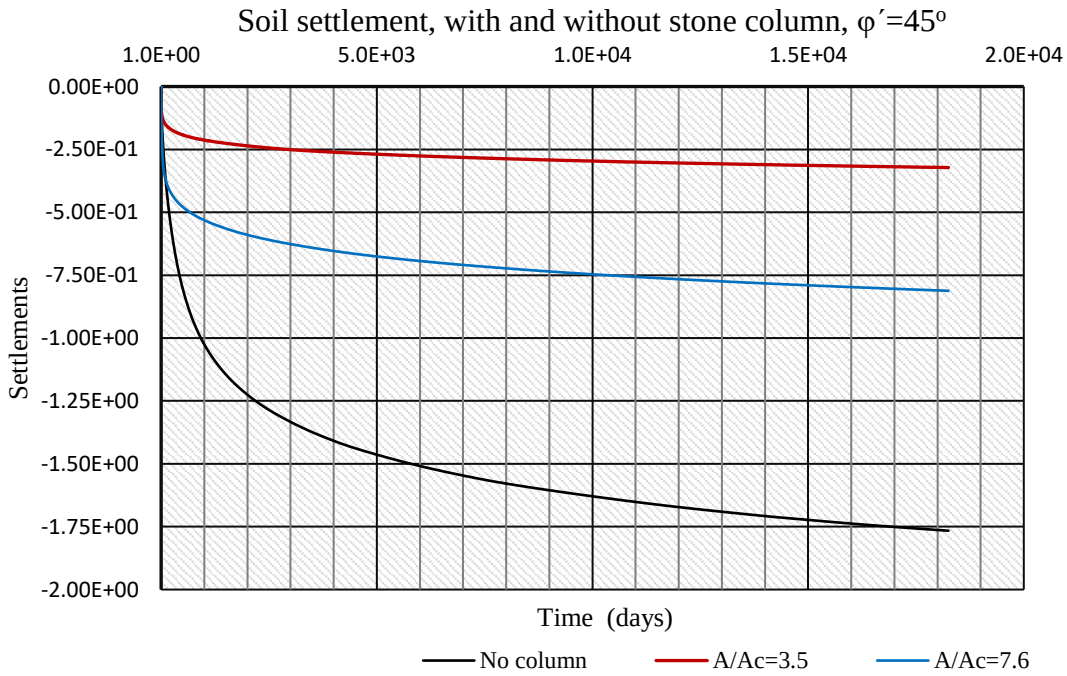

Figure 33: Comparison of settlement period for untreated and treated extremely soft clay.

Figure 34 shows the influence of lateral earth pressure K_0 value on the reinforcement soil settlements. As the input values of the model for K_0^{NC} and K_0 were obtained from the following equations (36, 37).

$$K_0^{NC} = 1 - sin\,\varphi' \qquad \textit{Eq. (47)}$$

$$K_0 = K_0^{NC}\sqrt{OCR} \qquad \textit{Eq. (48)}$$

The diagram illustrates the effect of varying K_0 values on the results, with specific examples at K_0 values of 1 and 0.58. As K_0 increases, the improvement factor also increases. For instance, when K_0 increases from 0.58 to 1, soil settlement improves by approximately 7% when the replacement ratio is 3.1, but only by about 4% when the replacement ratio is 7.6. This suggests that the benefits of settlement improvement due to lateral earth pressure decrease as the area ratio increases, which is consistent with previous studies that have found that the increase in lateral earth pressure caused by stone column construction diminishes beyond around 4 to 8 times the radius.

Increasing K_0 positively affects soil stability, enabling it to withstand stresses more effectively during both the construction and loading phases of stone column installation.

(n) for K_0= 1 and 0.58 for (0.5, 1, 2, 10, 20, and 50 years) /φ′=45°

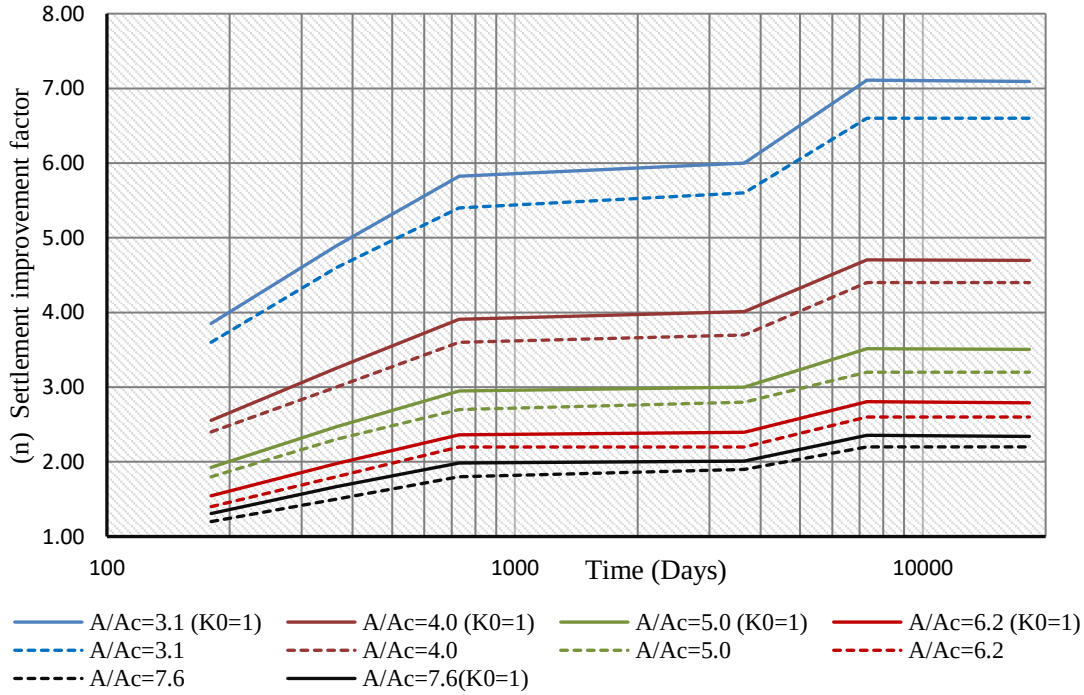

Figure 34: The variation in the improvement factor because of the K_0 value adjustment over different time intervals with an effective friction angle of 45°.

Figure 35 highlights the refinement of the mesh at the stone column boundaries, which reveals a region of stress concentration. Since the stone column has a higher capacity than the surrounding soil, this disparity increases stress in the stone column compared to the soil. As a result, stress concentration occurs within the stone column. The stress ratio in the soil surrounding the stone column to the stress in the stone column itself is referred to as the stress concentration factor, denoted as n_s.

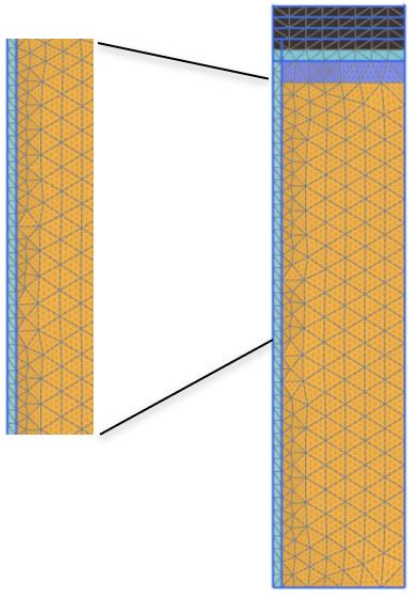

Figure 35: Mesh refinement where the stress is concentrated.

The following figure 36 shows the plastic points in the stone column and the active area of the soil surrounding the stone columns. It indicates that when the replacement ratio decreases and the effective friction angle increases, the stresses in the stone column increase, which increases the yielding points in stone column.

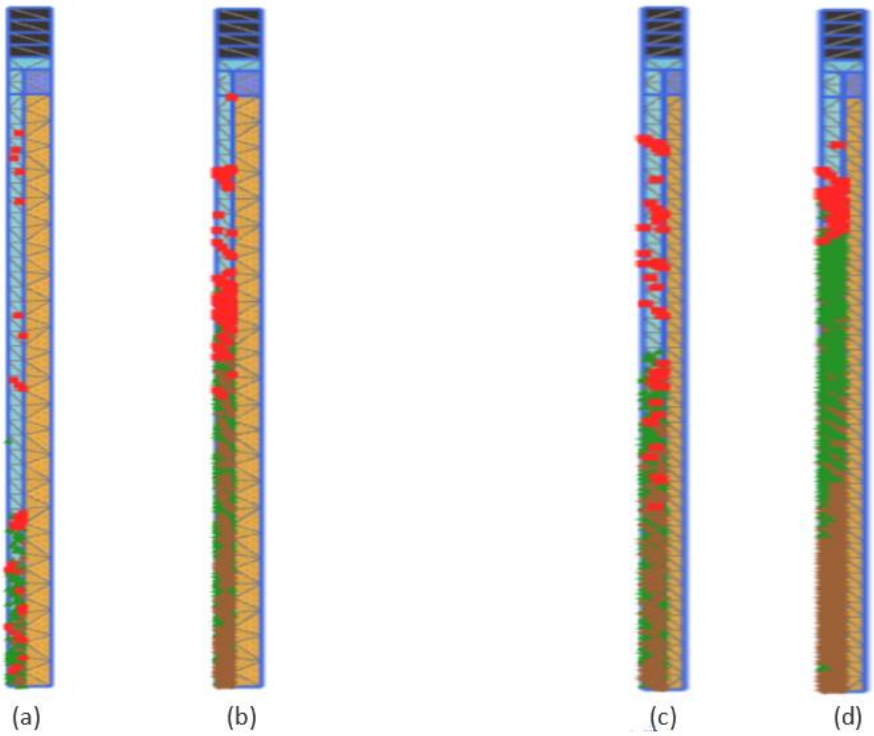

Figure 36: The plastic points in stone columns are illustrated as the following (a) and (b) show the results for a replacement ratio of 7.6, with effective friction angles of 37.5° and 45°, respectively; (c) and (d) display the results for a replacement ratio of 3.5, with the same arrangement of effective friction angles (37.5° and 45°).

6.2.2. Results of Soft Soil (SS) model

Like Creep-SCLAY1S, the following diagrams illustrate the changing of settlement improvement factor (n) with the change of the A/A_c ratio. See Figure 37.

The improvement factor in the Soft Soil constitutive model displays a similar trend to the Creep-SCLAY1S model. As the A/A_c ratio increases, the improvement factor decreases. Specifically, the improvement factor decreases by approximately 25% and 35% when the replacement ratio increases from 3.1 to 5 and 7.6, respectively, assuming a gravel effective friction angle is 45^o. Similarly, the settlement improvement factor is reduced by about 20%, 14%, and 15% for replacement ratios of 3.1, 5, and 7.6, respectively, when the effective friction angle of the stone column material decreases to 37.5^o.

However, the results obtained from the SS model show a significantly lower improvement factor, approximately one-third of that obtained from the Creep-SCLAY1S model.

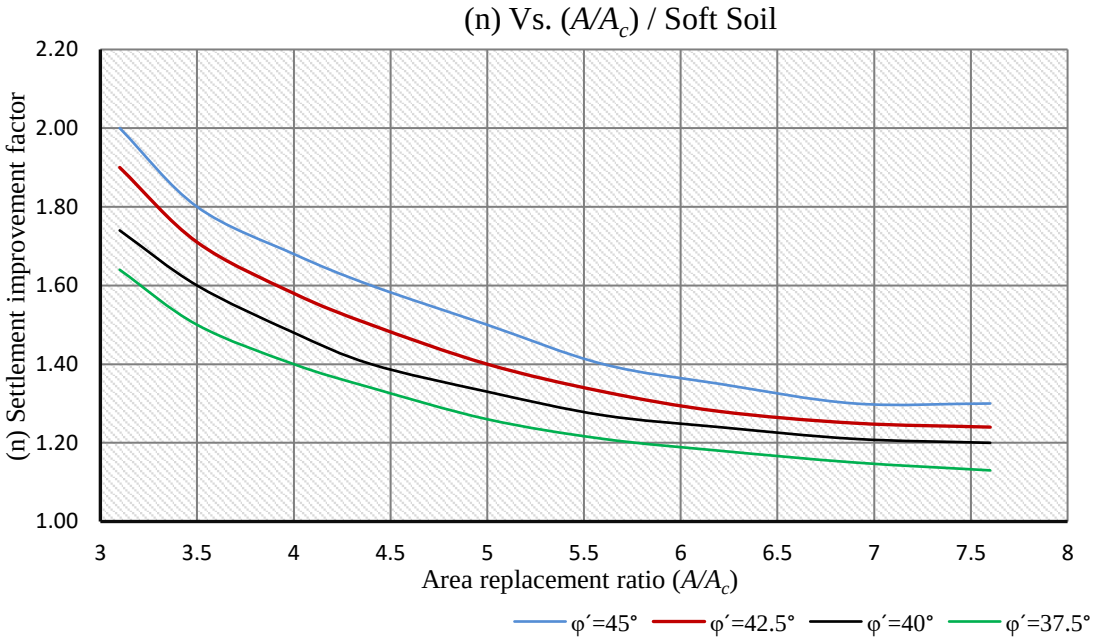

Figure 37: The correlation between the settlement improvement factor (n) and the A/Ac ratio with varying effective friction angles of the stone column.

The diagram in Figure 38 compares the results of this paper and those obtained from the study by Borges et al. (2009). The difference between both models is approximately 5%. This discrepancy may be attributed to differences in the length and diameter (5.5 and 1m) of the stone column in Borges et al. (2009) compared to the paper´s inputs, and variations in the soil parameters employed.

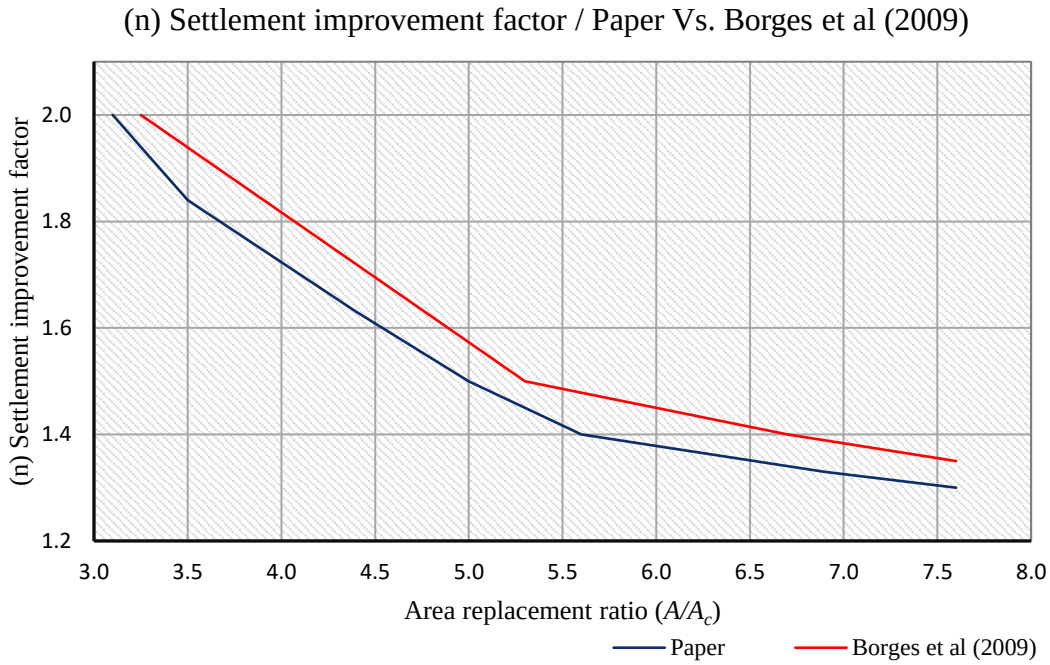

Figure 38: Comparison of the improvement factor results between the research paper and Borges et al., (2009).

6.2.3. Results of Soft Soil-creep (SSC) model

Similar to the prior models, Figures 39 and 40 depict the variation in settlement improvement factor (n) as the A/A_c ratio changes.

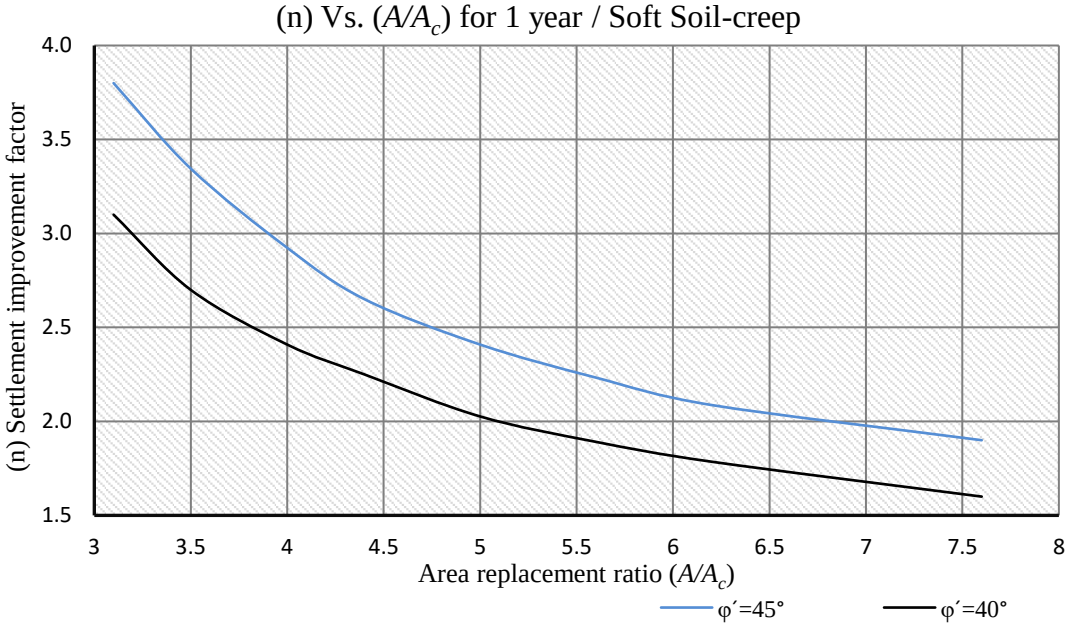

Figure 39: The correlation between the settlement improvement factor (n) and the A/A_c ratio for one-year time frame for two effective friction angles of the stone column.

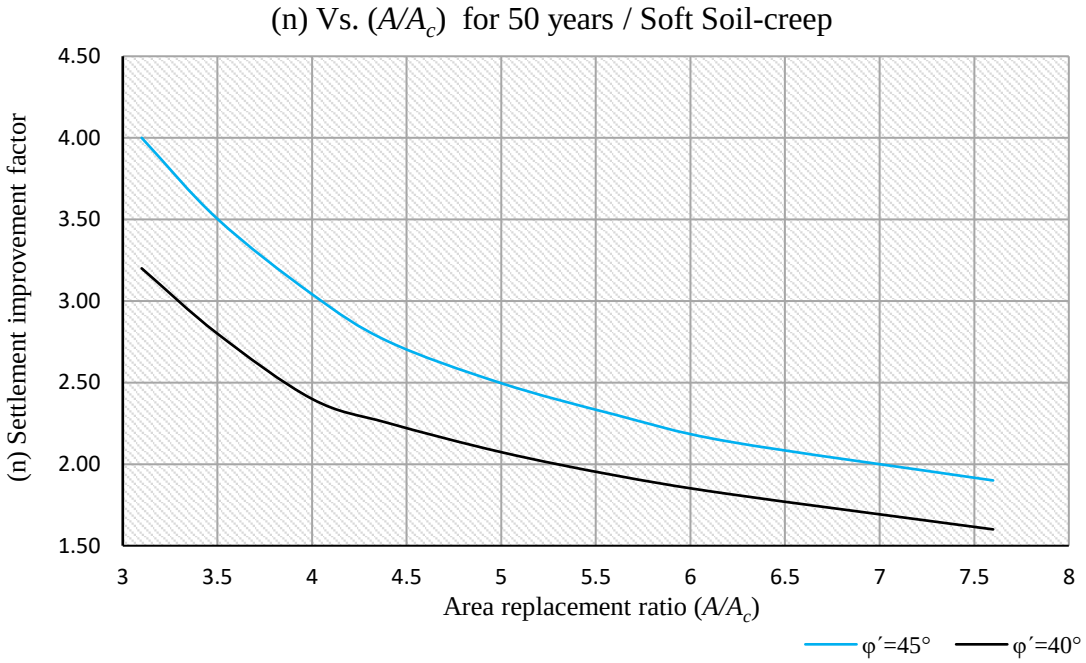

Figure 40:The correlation between the settlement improvement factor (n) and the A/Ac ratio of fifty-year time frame for two effective friction angles of the stone column.

The behaviour of soft soil under creep modelling is consistent with the previous soil models. When the effective friction angle of the column material decreases from 45° to 40°, the improvement factor drops by 18% and 20% at replacement ratios 3.1 at one year and 50 years, respectively. Additionally, the value of improvement factor value decreases by half when the replacement ratio increases from 3.1 to 7.6, regardless of the effective friction angle.

The comparison between the Soft Soil-creep (SSC) model and the Soft Soil (SS) model shows that the SSC model gives higher values for settlement improvement factor. This advantage is notable for both friction angles, with the SSC model exhibiting a 40-50% increase in improvement factor over the SS model for replacement ratios ranging from 3.1 to 5.6. However, this advantage diminishes to around 30% for replacement ratios above 6. See Figure 41. This highlights the significant contribution of creep to improving soil settlements when stone columns are employed.

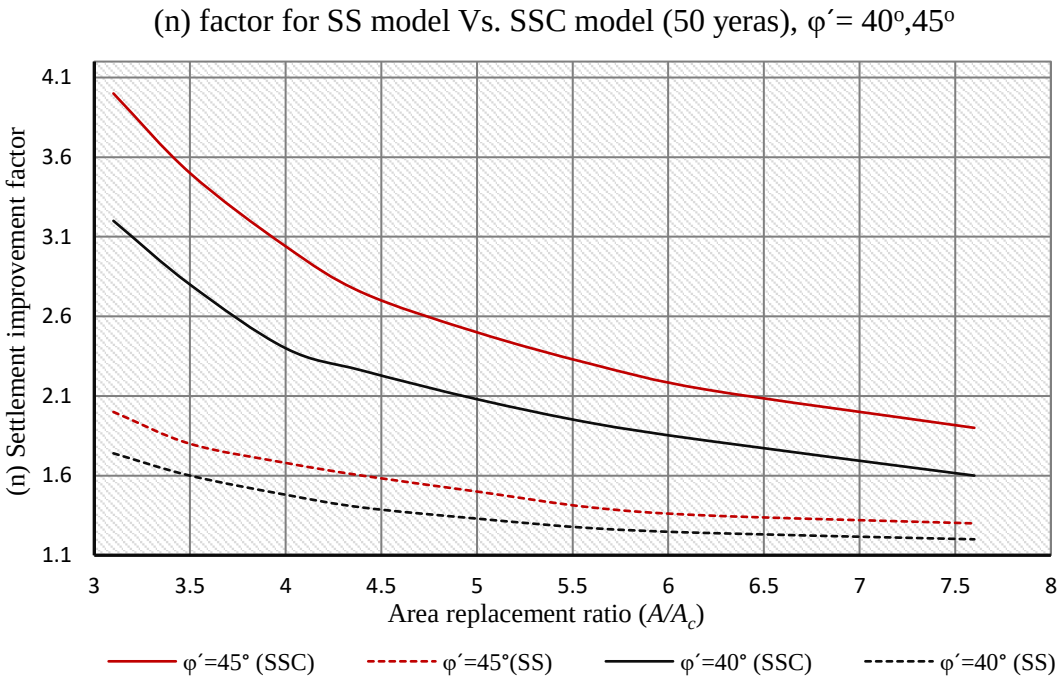

Figure 41: Settlement improvement factor comparison between SS model and SSC model (50 years and φ´=40º,45º)

6.2.4. Comparison of Priebe´s model and Models of paper

Figure 42 illustrates the difference between the Priebe´s stone column design diagrams and the models used in the thesis for 20 years time frame (i.e., when most of the improvement factors values become constant) and effective friction angle 45º.

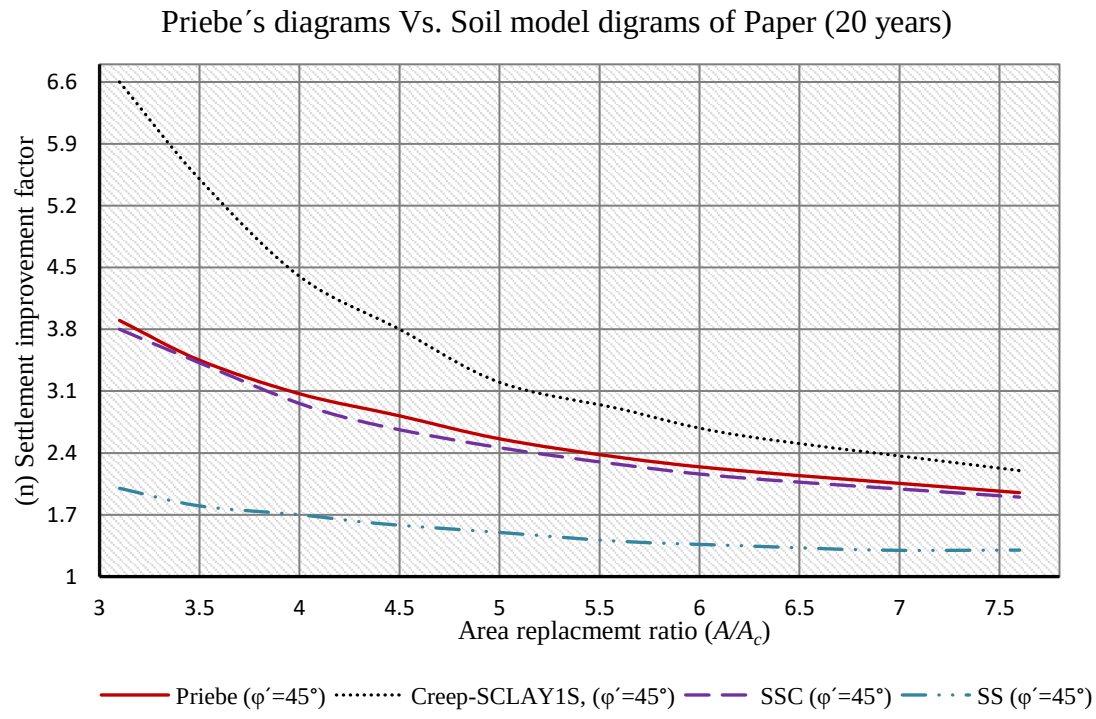

Figure 42: Result comparison between Priebe´s diagrams and paper´s models diagram for twenty-years time frame and effective friction angle (φ´=45º)

The Creep-SCLAY1S model predicts higher values for the improvement factor compared to Priebe's results. For a replacement ratio of 3.1, the Creep-SCLAY1S

model yields an improvement factor that is 41% higher than Priebe's, while this difference decreases to 25% and 20% for replacement ratios of 4.5 and 5.6, respectively. At a replacement ratio of A/A_c=7.6, the difference is only 11%. Similarly, the Soft Soil model shows improvement factors that are 48% and 40% less than those of Priebe's at replacement ratios of 3.1 and 5.6, respectively, with this difference decreasing to 33% at A/A_c=7.6. In contrast, the Soft Soil-Creep model shows settlement improvement factors that are only 4% less than those of Priebe's for all replacement ratios.

Figure 43 compares the results of Priebe´s model and paper´s models at effective friction angle of 40°.

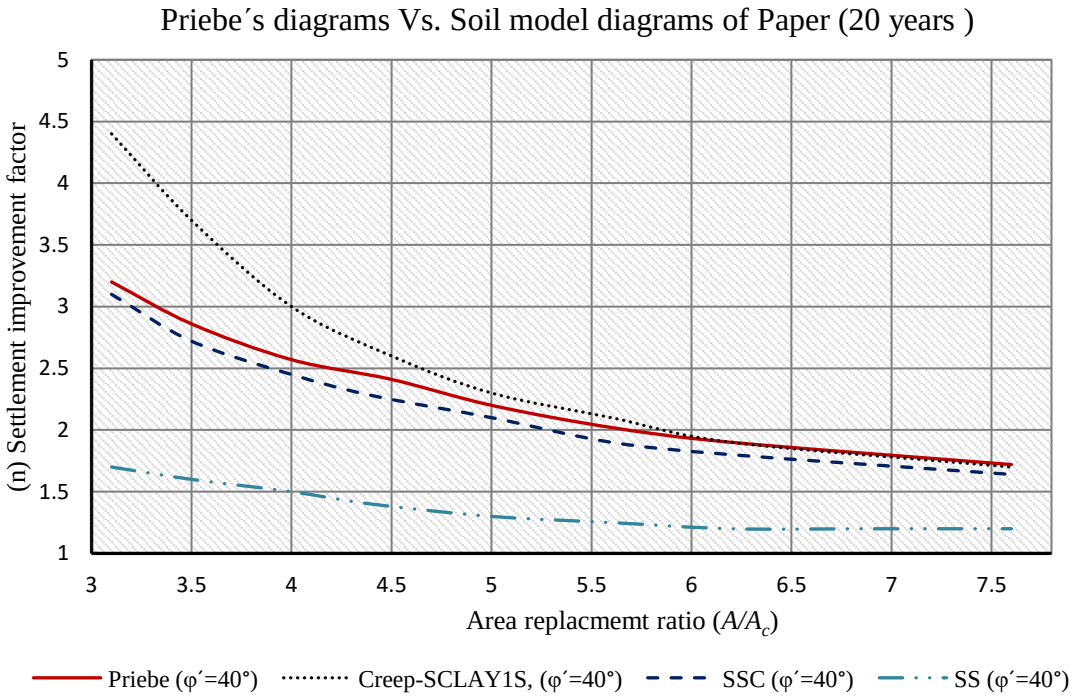

Figure 43: Result comparison between Priebe´s diagrams and paper´s models diagram for twenty-years time frame and effective friction angle (φ´=40°).

Like the previous diagram, the Soft Soil-creep model shows almost the same results as Priebe´s, with about 5% only. In comparison, the variations between the results of the Creep-SCLAY1S model and Priebe´s model decreased to about 27%, 23%, and 14% for replacement ratios 3.1, 3.5, and 4, respectively. At the same time, these variations were only about 4% for the rest of the replacement ratios. However, the variations between the Soft Soil model results and Priebe´s ones are still significant by about 47% and 44% for area replacement ratios of 3.1 and 3.5, respectively; this difference decreases to about 37% and 30% for 6.2 and 7.6 replacement ratios, respectively.

7. Conclusions and recommendations

Changing the constitutive model in numerical simulations can lead to significantly different settlement improvement factors, emphasizing the importance of selecting the most suitable model for the clay considered. Furthermore, incorporating creep increases the predicted improvement factor (n), highlighting the need to consider this factor in stone column design.

In addition, both the replacement ratio (A/A_c) and the effective friction angle of the stone column material have a significant impact on the improvement factor value. The (n) value decreases as the replacement ratio increases, and it becomes almost less than 2.0 for all models when it exceeds 7.6. Conversely, using stone column material with an effective friction angle of 45° or more can enhance the value of (n), while using gravel with an effective friction angle less than 45° can noticeably reduce the improvement factor.

Furthermore, lateral earth pressure plays a crucial role in soil stability and capacity, as an increase in K_0 reduces deformation of the loaded stone column.

On the other hand, for the Creep-SCLAY1S model, the length of the stone column has a significant impact on the settlement reduction factor. Increasing the length of the stone column increases the value of the settlement improvement factor; this improvement increases as the replacement ratio increases.

Interestingly, a notable disparity emerges when comparing Priebe's diagrams with the various models used, except for the Soft Soil-creep model. The Soft Soil-creep model gives almost the same results as Priebe for both effective friction angles (45^o and 40^o) considered. The results of the Soft Soil model predict significantly lower improvement factors than Priebe. This variation is between 47% and 30% for both friction angle values and all area replacement ratios. Creep-SCLAY1S gives higher improvement factor values than Priebe for an effective friction angle of 45°, while this variation decreases to almost vanish at a replacement ratio of 5 when the effective friction angle is 40^o. However, these discrepancies may be attributed to variations in input parameters.

Finally, applying stone columns in extremely soft soil should consider the issues that may arise during installation, in addition to choosing the suitable model and parameters. All these factors can significantly influence the predicted settlement improvement factors.

Recommendation:

- As the stone column construction increases the lateral earth pressure of the surrounding soil, it is crucial to consider its effect on the settlement improvement factor.
- Practical tests are required to check the potential of applying Pribes' diagram for various soil types.
- The complexity of stone column in very soft soils is underscored by the significant impact of various input parameters on the reduction settlement factor, necessitating the exploration of these impacts through more models.

8. Reference

Abdelkrim, M., & De Buhan, P. (2007). An elastoplastic homogenization procedure for predicting the settlement of a foundation on a soil reinforced by columns. *European Journal of Mechanics - a/Solids*, *26*(4), 736–757. https://doi.org/10.1016/j.euromechsol.2006.12.004

Almeida, M. S. S., Marques, M. E. S., Filho, M. R., De Freitas Fagundes, D., Lima, B. T., Polido, U., Cirone, A., & Hosseinpour, I. (2022). Ground improvement techniques applied to very soft clays: state of knowledge and recent advances. *Soils & Rocks*, *46*(1), e2023008222. https://doi.org/10.28927/sr.2023.008222

Babu, M. R. D., Nayak, S., & Shivashankar, R. (2012). A critical review of construction, analysis and behaviour of stone columns. *Geotechnical and Geological Engineering*, *31*(1), 1–22. https://doi.org/10.1007/s10706-012-9555-9

Balaam, N. P., & Booker, J. R. (1981). Analysis of rigid rafts supported by granular piles. *International Journal for Numerical and Analytical Methods in Geomechanics*, *5*(4), 379–403. https://doi.org/10.1002/nag.1610050405

Barksdale, R. D., & Bachus, R. C. (1983). *DESIGN and CONSTRUCTION of STONE COLUMNS VOL.I* (FHWAIRD-83/026). https://rosap.ntl.bts.gov/view/dot/25319/dot_25319_DS1.pdf

Basack, S., Indraratna, B., & Rujikiatkamjorn, C. (2016). Analysis of the behaviour of Stone Column Stabilized soft ground supporting transport infrastructure. *Procedia Engineering*, *143*, 347–354. https://doi.org/10.1016/j.proeng.2016.06.044

Berre, T. (2014). Test fill on soft plastic marine clay at Onsøy, Norway. *Canadian Geotechnical Journal*, *51*(1), 30–50. https://doi.org/10.1139/cgj-2012-0479

Berre, T. (2018). Test fill brought to failure on soft plastic marine clay at Onsøy, Norway. *Canadian Geotechnical Journal*, *55*(4), 563–576. https://doi.org/10.1139/cgj-2017-0078

Borges, J. L., Domingues, T. S., & Cardoso, A. S. (2009). Embankments on Soft Soil Reinforced with Stone Columns: Numerical Analysis and Proposal of a New Design Method. *Geotechnical and Geological Engineering*, *27*(6), 667–679. https://doi.org/10.1007/s10706-009-9266-z

Buismann, K. (1936). Results of long duration settlement tests. In *Proceedings 1st International Conference on Soil Mechanics and Foundation Engineering.* Volume 1, Cambridge, Massachusetts, pp. 103-1.07

Butterfield, R. (1979). A natural compression law for soils (an advance on e–log p′). *Géotechnique/Geotechnique*, *29*(4), 469–480. https://doi.org/10.1680/geot.1979.29.4.469

Camelo, C. Y. S. (2016). THREE-DIMENSIONAL NUMERICAL ANALYSIS OF A TEST EMBANKMENT ON GEOSYNTHETIC-ENCASED STONE COLUMNS (Doctoral dissertation, Universidade Federal do Rio de Janeiro).

Carvajal, E. P. P., Vukoti, G., Castro, J. V., & Wehr, W. (2013). Comparison between theoretical procedures and field test results for the evaluation of installation effects of vibro-stone columns. In *CRC Press eBooks* (pp. 205–211). https://doi.org/10.1201/b13890-30

Castro, J. V. (2014). Numerical modelling of stone columns beneath a rigid footing. *Computers and Geotechnics*, *60*, 77–87. https://doi.org/10.1016/j.compgeo.2014.03.016

Castro, J. V., Cimentada, A., Da Costa, A., Cañizal, J., & Sagaseta, C. (2013). Consolidation and deformation around stone columns: Comparison of theoretical and laboratory results. *Computers and Geotechnics*, *49*, 326–337. https://doi.org/10.1016/j.compgeo.2012.09.004

Castro, J. V. (2017). Modelling stone columns. *Materials*, *10*(7), 782. https://doi.org/10.3390/ma10070782

Castro, J. V., & Karstunen, M. (2010). Numerical simulations of stone column installation. *Canadian Geotechnical Journal*, *47*(10), 1127–1138. https://doi.org/10.1139/t10-019

Castro, J. V., & Sagaseta, C. (2009). Consolidation around stone columns. Influence of column deformation. *International Journal for Numerical and Analytical Methods in Geomechanics*, *33*(7), 851–877. https://doi.org/10.1002/nag.745

Chu, J., Varaksin. S., Klotz, U., and Menge, P. (2009). "Construction Processes, State of the Art Report." *17th International Conference on Soil Mechanics and Geotechnical Engineering,* Alexandria, Egypt, 5-9 October 2009

Dash, S. K., & Bora, M. C. (2013). Improved performance of soft clay foundations using stone columns and geocell-sand mattress. *Geotextiles and Geomembranes*, *41*, 26–35. https://doi.org/10.1016/j.geotexmem.2013.09.001

Deshpande, T. D., Kumar, S. R., Begum, G., Basha, S. a. K., & Rao, B. H. (2021). Analysis of Railway Embankment Supported with Geosynthetic-Encased Stone Columns in Soft Clays: A Case Study. *International Journal of Geosynthetics and Ground Engineering*, *7*(2). https://doi.org/10.1007/s40891-021-00288-5

Elshazly, H. A., Hafez, D. H., & Mossaad, M. (2006). Back-calculating vibro-installation stresses in stone-column-reinforced soils. *Proceedings of the Institution of Civil Engineers*, *10*(2), 47–53. https://doi.org/10.1680/grim.2006.10.2.47

Elshazly, H. A., Hafez, D. H., & Mossaad, M. (2008). Reliability of conventional settlement Evaluation for circular foundations on stone columns. *Geotechnical and Geological Engineering*, *26*(3), 323–334. https://doi.org/10.1007/s10706-007-9169-9

Elshazly, H., Elkasabgy, M., & Elleboudy, A. (2005). *Assessment of alterations to K_0 during stone columns installation using test data and cavity expansion solution*. Inter. Conf. On Tsunami Reconstruction with Geosynthetics – Protection, Mitigation and Rehabilitation of Coastal and Waterway Erosion Contro, Bangkok, Thailand.

Emam, E., Youssef, A., & Abdelgalil, A. (2022). Effect of encasement on the behaviour of granular piles. *ERJ. Engineering Research Journal*, *45*(1), 65–76. https://doi.org/10.21608/erjm.2022.100585.1117

Gaber, M., Kasa, A., Rahman, N. A., & Alsharef, J. M. (2018). Comparison between unit cell and plane strain models of stone column ground improvement. *International Journal of Engineering & Technology*, *7*(2), 263. https://doi.org/10.14419/ijet.v7i2.8797

Gaber, M., Kasa, A., Abdul-Rahman, N., & Alsharef, J. (2018). Simulation of stone column ground improvement (Comparison between axisymmetric and plane strain). *American Journal of Engineering and Applied Sciences*, *11*, 129–137. https://doi.org/10.3844/ajeassp.2018.129.137

Gens, A., Nova, R., International Society for Soil Mechanics and Foundation Engineering; French Committee, & International Society for Soil Mechanics and Foundation Engineering; Hellenic Society. (1993). Conceptual bases for a constitutive model for bonded soils and weak rocks. In Vols 1-3 (pp. 485-494). A Balkema.

Golakiya, H. D., & Lad, M. D. (2015). GROUND IMPROVEMENT BY USING STONE COLUMNS. *JETIR*, *Volume 2*(Issue 11). https://www.jetir.org/papers/JETIR1511023.pdf

Goughnour, R. R., & Bayuk, A. A. (1979). A field study of long-term settlements of loads supported by stone columns in soft ground. In *Geosyntheticssociety*. International Conference on Soil Reinforcement: Reinforced Earth and Other Techniques, Paris. Vol 1 (pp. 279-285).

Greenwood, D. A. (1970) Mechanical improvement of soils below ground surface. In: Conference on Ground Engineering. London, Institute of Civil Engineering. pp. 11-22.

Grizi, A., Al-Ani, W., & Wanatowski, D. (2022). Numerical Analysis of the Settlement Behaviour of Soft Soil Improved with Stone Columns. *Applied Sciences*, *12*(11), 5293. https://doi.org/10.3390/app12115293

Guéguin, M., Hassen, G., & De Buhan, P. (2015). Stability analysis of homogenized stone column reinforced foundations using a numerical yield design approach. *Computers and Geotechnics*, *64*, 10–19. https://doi.org/10.1016/j.compgeo.2014.11.001

Guetif, Z., Bouassida, M., & Debats, J. (2007). Improved soft clay characteristics due to stone column installation. *Computers and Geotechnics*, *34*(2), 104–111. https://doi.org/10.1016/j.compgeo.2006.09.008

Guo, R., & Li, G. (2008). Elasto-plastic constitutive model for geotechnical materials with strain-softening behaviour. *Computers & Geosciences*, *34*(1), 14–23. https://doi.org/10.1016/j.cageo.2007.03.012

Hernvall, H., Karlsson, M., Dijkstra, J., & Karstunen, M. (n.d.). *Impact of rate-dependency on the stability of ØNSOY Test 1 Embankment*. Chalmers University of Technology.

Hu, W. (1995) Physical modelling of group behaviour of stone column foundations. Ph.D. dissertation, University of Glasgow, Glasgow, U.K., 313 pp.

Idrus, J., Ng, K. S., Nujid, M. M., & Abdullah, N. H. H. (2023). A review of stone columns performance in soft soils. *AIP Conference Proceedings*. https://doi.org/10.1063/5.0111958.

Jakati, S., Joshi, A., & Kolekar, Y. A. (2019). A Comparative Study of Design and Construction Practice of Stone Column. In *Lecture notes in civil engineering* (pp. 359–368). https://doi.org/10.1007/978-981-13-6713-7_28.

Jellali, B., Bouassida, M., & De Buhan, P. (2005). A homogenization method for estimating the bearing capacity of soils reinforced by columns. *International Journal for Numerical and Analytical Methods in Geomechanics*, *29*(10), 989–1004. https://doi.org/10.1002/nag.441

Juran, I., & Guermazi, A. (1988). SETTLEMENT RESPONSE OF SOFT SOILS REINFORCED BY COMPACTED SAND COLUMNS. *Journal of Geotechnical Engineering*, *Volume 114*(Issue 8).

https://doi.org/10.1061/(ASCE)0733-9410(1988)114:8(930)
Kavvadas, M., & Amorosi, A. (2000). A constitutive model for structured soils. *Géotechnique/Geotechnique*, *50*(3), 263–273. https://doi.org/10.1680/geot.2000.50.3.263
Kelln, C., Sharma, J., Hughes, D., & Graham, J. (2008). An improved elastic–viscoplastic soil model. *Canadian Geotechnical Journal*, *45*(10), 1356–1376. https://doi.org/10.1139/t08-057
Kok, Sien & Ti, & Huat, Bujang & Noorzaei, Jamaloddin & Jaafar, Saleh. (2009). A Review of Basic Soil Constitutive Models for Geotechnical Application. Electronic Journal of Geotechnical Engineering. 14.
Koskinen, M., Karstunen, M.& Wheeler, S., 2002. Modelling destructuration and anisotropy of a soft natural clay, In: *5th European Conference on Numerical Methods in Geotechnical Engineering*. Presses de l'ENPC, Paris, pp. 11–20.
Madhav, M. R., & Vitkar, P. P. (1978). Strip footing on weak clay stabilized with a granular trench or pile. *Canadian Geotechnical Journal*, *15*(4), 605–609. https://doi.org/10.1139/t78-066
Malarvizhi, S & Ilamparuthi, K. (2004). Load versus settlement of clay bed stabilized with stone & reinforced stone columns.
Malarvizhi, S., & Ilamparuthi. (2007). Comparative study on the behaviour of encased stone column and conventional stone column. *Soils and Foundations*, *47*(5), 873–885. https://doi.org/10.3208/sandf.47.873
McCabe, B. A., Nimmons, G. J., & Egan, D. (2009). A review of field performance of stone columns in soft soils. *Proceedings of the Institution of Civil Engineers*, *162*(6), 323–334. https://doi.org/10.1680/geng.2009.162.6.323
McCabe, B. A. (2014). *The influence of Creep on the settlement of foundations supported by stone columns* [PhD dissertation, University of Galway]. https://www.researchgate.net/publication/272563053_The_influence_of_creep_on_the_settlement_of_foundations_supported_by_stone_columns
McKenna, J. M., Eyre, W. A., & Wolstenholme, D. R. (1975). Performance of an embankment supported by stone columns in soft ground. *Geotechnique*, *25*(1), 51–59. https://doi.org/10.1680/geot.1975.25.1.51
Mecsi, J. (2013) Geotechnical Engineering Examples and Solutions Using the Cavity Expansion Theory. Budapest, Hungary, Geotechnical Society, 232 pp
Mitchell, J. K. (1981). *Soil Improvement: State of the Art Report*. https://www.issmge.org/publications/publication/soil-improvement-state-of-the-art-report
Neher, H. P., & Wehnert, M. (n.d.). *An evaluation of soft soil models based on trial embankments*. Computer Methods and Advances in Geomechanics: Proceedings of the 10th International Conference on Computer Methods and Advances in Geomechanics, Tuscon, Arizona, United States of America. https://vdocuments.mx/an-evaluation-of-soft-soil-models-based-on-trial-embankments-neher-2001.html?page=1
Ng, K. S., & Tan, S. (2014). Stress transfer mechanism in 2D and 3D unit cell models for stone column improved ground. *International Journal of Geosynthetics and Ground Engineering*, *1*(1). https://doi.org/10.1007/s40891-014-0003-1
Ng, K. S., & Tan, S. (2015). Simplified homogenization method in stone column designs. *Soils and Foundations*, *55*(1), 154–165. https://doi.org/10.1016/j.sandf.2014.12.012
Nova, R., Castellanza, R., & Tamagnini, C. (2003). A constitutive model for bonded geomaterials subject to mechanical and/or chemical degradation. *International*

Journal for Numerical and Analytical Methods in Geomechanics, *27*(9), 705–732. https://doi.org/10.1002/nag.294

Pal, S., & Deb, K. (2019). Effect of clogging of stone column on drainage capacity during soil liquefaction. *Soils and Foundations*, *59*(1), 196–207. https://doi.org/10.1016/j.sandf.2018.10.005

Piccinini, Isabela. (2015). Ground Improvement with Stone Columns - Methods of Calculating Settlement Improvement Factor. 10.13140/RG.2.1.2159.2486.

Pietraszewska, D. K. (2011). *Numerical modelling of soft soils improved with stone columns* [Dissertation, University of Strathclyde]. https://stax.strath.ac.uk/concern/theses/d217qp58s

Potts, D. M., & Zdravkovic, L. (1999). *Finite element analysis in geotechnical engineering*. ICE Publishing. http://www.t-telford.co.uk

Prakash, K., & Krishnamoorthy, A. (2022). Effectiveness of stone and deep mixing lime columns on stability of embankments constructed on soft consolidating soil. *Geotechnical and Geological Engineering*, *41*(1), 533–552. https://doi.org/10.1007/s10706-022-02269-5

Prasad, S., & PVV, S. (2016). Improvement of Soft Soil Performance using Stone Columns Improved with Circular Geogrid Discs. *Indian Journal of Science and Technology*, *9*(30). https://doi.org/10.17485/ijst/2016/v9i30/99186

Ranjan, G. (2016). Ground Treated with Granular piles and its Response Under Load https://www.igs.org.in/storage/annual-lecture/annual-lecture-1988-180523064611.pdf

Sarvaiya, H. K., & Solanki, C. H. (2015). AN EXPERIMENTAL STUDY ON LOAD CAPACITY OF FLOATING STONE COLUMN IN SOFT SOIL. *Nternational Journal of Advances in Engineering & Technology*, *ISSN: 22311963*. https://www.ijaet.org/media/9I30-IJAET0830216-v8-iss6-pp965-975.pdf

Schaefer, V. R., Berg, R. R., Collin, J. G., Christopher, B. R., DiMaggio, J. A., Filz, G. M., Bruce, D. A., & Ayala, D. (2016). *Ground Modification Methods Reference Manual – Volume I* (FHWA-NHI-16-027). https://www.fhwa.dot.gov/engineering/geotech/pubs/nhi16027.pdf

Schaefer, V. R., Mitchell, J. K., Berg, R. R., Filz, G. M., & Douglas, S. C. (2012). Ground Improvement in the 21st Century: A Comprehensive Web-Based Information System. *Ascelibrary*. https://doi.org/10.1061/9780784412138.0011

Sexton, B. G., McCabe, B. A., & Castro, J. V. (2013). Appraising stone column settlement prediction methods using finite element analyses. *Acta Geotechnica*, *9*(6), 993–1011. https://doi.org/10.1007/s11440-013-0260-5

Shahu, J. T., & Reddy, Y. R. (2011). Clayey Soil Reinforced with Stone Column Group: Model Tests and Analyses. *Journal of Geotechnical and Geoenvironmental Engineering*, *137*(12). https://doi.org/10.1061/(ASCE)GT.1943-5606.00005

Shehata, H. F., Sorour, T., & Fayed, A. L. (2018). Effect of stone column installation on soft clay behavior. *International Journal of Geotechnical Engineering*, *15*(5), 530–542. https://doi.org/10.1080/19386362.2018.1478245

Shien, N. K. (2013). Cavity expansion approach in modelling stone column installation effect. *Engineering, Environmental Science*. https://doi.org/10.13140/2.1.4240.8649

Sivasithamparam, N., Karstunen, M., & Bonnier, P. (2015). Modelling creep behaviour of anisotropic soft soils. *Computers and Geotechnics*, *69*, 46–57. https://doi.org/10.1016/j.compgeo.2015.04.015

Sondermann, W., Raju, V. R., Daramalinggam, J., & Yohannes, M. (Eds.). (2016). *Practical design of Vibro stone columns*. https://www.researchgate.net/publication/335274285_Practical_Design_of_Vibro_Stone_Columns

Stuedlein, A. W., & Holtz, R. D. (2013). Bearing capacity of spread footings on aggregate pier reinforced clay. *Journal of geotechnical and geoenvironmental engineering*, *139*(1), 49-58.

Tai, P., & Zhou, C. (2019). Effects of Clogging on Settlement Predictions of Ground Improved with Stone Columns. *KSCE Journal of Civil Engineering*, *23*(9), 3889–3896. https://doi.org/10.1007/s12205-019-2414-y

Tan, S. & Tjahyono, Sindhu & Oo, Krisnanto. (2008). Simplified Plane-Strain Modelling of Stone-Column Reinforced Ground. Journal of Geotechnical and Geoenvironmental Engineering - J GEOTECH GEOENVIRON ENG. 134. 10.1061/(ASCE)1090-0241(2008)134:2(185).

Van Impe, W.Y. and E. De Beer, 1983. Improvement of settlement behaviour of softy layers by means of stone columns. Proceedings of the 8th International Conference on SMFE, (SMFE' 83), Helsinki, pp: 309-312.

Vesić, A.S. (1972). Expansion of Cavities in Infinite Soil Mass. *Journal of the Soil Mechanics and Foundations Division, 98*, 265-290.

Wassie, T. A., & Demir, G. (2023). Behavior of an embankment on stone Column-Reinforced soft soil. *Slovak Journal of Civil Engineering*, *31*(4), 9–15. https://doi.org/10.2478/sjce-2023-0022

Watts, K.S., Johnson, D., Wood, L.A. & Saadi, A. 2000. An instrumented trial of vibro ground treatment supporting strip foundations in a variable fill. Géotechnique 50(6): 699-708

Weber, T., Springman, S. M., Gäb, M., Račanský, V., & Schweiger, H. (2008). Numerical modelling of stone columns in soft clay under an embankment. In *Taylor & Francis eBooks* (pp. 305–311). https://doi.org/10.1201/9780203883334.ch39

Wehr, J. (2013). The undrained cohesion of the soil as a criterion for column installation with a depth vibrator. In *CRC Press eBooks* (pp. 241–244). https://doi.org/10.1201/b13890-35

Wehr, J., Eckert, M., Dahlström, M., & Topolnicki, M. (2008). *Stone columns in very soft clays in Sweden* [Authors]. 11th Baltic Sea Geotechnical Conference, Gdansk, Poland.

Welsh, J., Warren, J., & Lukas, R. (200 C.E.). *Ground Improvement Technical Summaries: Volume 2* (FHWA-SA-98-086 R). https://rosap.ntl.bts.gov/view/dot/41760

Wood, D. M., Hu, W., & Nash, D. (2000). Group effects in stone column foundations: model tests. *Géotechnique/Geotechnique*, *50*(6), 689–698. https://doi.org/10.1680/geot.2000.50.6.689

Zentar, R., Karstunen, M. and Wheeler, S. (2002) Influence of anisotropy and destructuration on undrained shearing of natural clays. In: 5th European Conference on Numerical Methods in Geotechnical Engineering, Paris, France, 4-6 September, pp. 21-26. ISBN 2-85978-362-8